

**Remote sensing of impervious surfaces growth:
A framework for quantifying urban expansion and re-densification mechanisms based on the remotely sensed
data**

AmirReza Shahtahmassebi^{1*}, Jie Song¹, Qing Zheng¹, George Alan Blackburn², Ke Wang¹,
Ling Yan Huang¹, Yi Pan¹, Nathan Moore³, Golnaz Shahtahmassebi⁴, Reza Sadrabadi Haghighi⁵
,Jing Song Deng¹

¹*Institute of Agriculture Remote Sensing and Information Technology, College of Environment and Natural Resource, Zhejiang University, Hangzhou 310058, China*

²*Lancaster Environment Centre, Lancaster University, Lancaster LA1 4YQ, UK*

³*Department of Geography, Michigan State University, East Lansing, MI, USA,48823*

⁴*College of Arts and Science, School of Science & Technology, Nottingham Trent University, UK*

⁵*Department of Agronomy and Plant Breeding, Mashhad Branch, Islamic Azad University, Iran*

Telephone: 0086571-88982272

*Corresponding author: amir511@zju.edu.cn; kwang@zju.edu.cn

Abstract

A substantial body of literature has accumulated on the topic of using remotely sensed data to map impervious surfaces which are widely recognized as an important indicator of urbanization. However, the remote sensing of impervious surface growth has not been successfully addressed. This study proposes a new framework for deriving and summarizing urban expansion and re-densification using time series of impervious surface fractions (ISFs) derived from remotely sensed imagery. This approach integrates multiple endmember spectral mixture analysis (MESMA), analysis of regression residuals, spatial statistics (Getis_Ord) and urban growth theories; hence, the framework is abbreviated as MRGU. The performance of MRGU was compared with commonly used change detection techniques in order to evaluate the effectiveness of the approach. The results suggested that the ISF regression residuals were optimal for detecting impervious surface changes while Getis_Ord was effective for mapping hotspot regions in the regression residuals image. Moreover, the MRGU outputs agreed with the mechanisms proposed in several existing urban growth theories, but importantly the outputs enable the refinement of such models by explicitly accounting for the spatial distribution of both expansion and re-densification mechanisms. Based on Landsat data, the MRGU is somewhat restricted in its ability to measure re-densification in the urban core but this may be improved through the use of higher spatial resolution satellite imagery. The paper ends with an assessment of the present gaps in remote sensing of impervious surface growth and suggests some solutions. The application of impervious surface fractions in urban change detection is a stimulating new research idea which is driving future research with new models and algorithms.

Keywords: Impervious surface; Regression residuals; Getis_Ord; Re-densification; Expansion; MESMA; ISF.

1. Introduction

Remote sensing of impervious surfaces has been the subject of research in urban remote sensing in recent years partly because it is an indicator of the degree of urbanization, and partly because it is a major indicator of environmental quality (Weng, 2012). Growth of impervious surfaces (e.g. via the construction of highways, industrial regions and residential areas) presents serious challenges in terms of the environment, climate, urban planning, population health and natural resources (Elvidge et al., 2007; Parece and Campbell, 2013). Timely and accurate information about the spatial distribution of impervious surface changes will, thus, be a key resource for dealing with such challenges and it needs to be applicable to the diversity of the world's urban areas.

Since the 1970s, airborne and satellite sensor imagery have been utilized for mapping impervious surfaces and its changes (Weng 2012). The earlier techniques for impervious surface change detection from remotely sensed imagery were based on the comparison of spectral responses (e.g. image to image comparison or map to map comparison (Yang and Liu, 2005; Lu et al., 2011)). These techniques detect the conversion of pervious lands into impervious surfaces at the pixel level, i.e. between-class changes. About two decades ago, researchers began to realize that such methods could not identify sub-pixel changes (i.e. within-class changes or re-densification) of impervious surfaces (Ridd, 1995). In addition, the presence of mixed pixels within urban landscapes can adversely affect the performance of traditional techniques (Wu et al., 2003). This is a common problem in images with medium spatial resolution imagery (e.g. Landsat ETM+)(Demarchi et al., 2012).

The existence of these two problems led to the development of a sub-pixel framework. This framework emphasizes that quantification should be employed for monitoring change in impervious surfaces in order to preserve heterogeneity of impervious surface land cover, characterize impervious surface land cover independent from analyst-imposed definitions, and more accurately capture change through time (Ridd, 1995; Mather, 1999; Weng and Lu, 2009). This framework can be broken down into two main stages. Firstly, sub-pixel approaches are used to estimate the proportion of impervious surface within each pixel (i.e. impervious surface fraction, ISF). Examples of sub-pixel techniques applied to remotely sensed imagery include regression (Yang and Liu, 2005), regression trees (Yang et al., 2003; Xian, 2007), neural networks (Sun et al., 2011), spectral mixture analysis (Wu and Murray, 2003) and multiple endmember spectral mixture analysis (MESMA) (Rashed et al., 2003). Reviews of these techniques have been given by Slonecker et al. (2001) and Weng (2012). Secondly, the outputs from the sub-pixel techniques (ISFs) are subjected to change detection analysis, which is focus of this paper.

In most cases, change-detection based on impervious surface fraction images is appropriate and informative since it measures between-class change, within-class change and degree of urbanization in conjunction with environmental quality (Ridd, 1995). Understanding the spatial distribution of between-class change and within-class change reveals comprehensive information about urban expansion, infilling, re-densification and historical concentric urban rings. This is because between-class change generally occurs around existing settlements or in formerly open spaces within urbanized areas, thus promoting urban expansion and infilling, respectively. By contrast, within-class change is associated with modification and transformation of physical structures in urban land covers that cause urban re-densification. Such information would be crucial for quantifying the consequences of impervious surface growth such as loss of biodiversity, urban heat island development and air pollution.

Having these potential advantages, a considerable number of studies has suggested different techniques to quantify changes in impervious surface fractions (ISFs), however, assessing and comparing this body of literature is very difficult. A selection of these methods is furnished in Table 1, which does not attempt a comprehensive review, but rather provides an overview of the variety of algorithms. The impervious surface change detection methods can be grouped into four categories: (1) Hybrid techniques, in which impervious surface changes are analyzed by integrating different approaches such as visual interpretation, rule-based methods along with pixel by pixel comparison and Change Vector Analysis(CVA). Hybrid techniques are also generally based on two dates of imagery; (2)Time series analysis, in which changes in impervious surfaces over time (more than two dates) are monitored based on multi-date classification, write memory function and per pixel level comparison; (3) Modeling, in which modifications of impervious surfaces are modeled using mathematical and statistical approaches; (4) Spatial metrics, in which patterns of change in impervious surfaces are revealed using impervious surface spatial metrics such as percent connected impervious surface area(Wu and Thompson,2013).

Table 1

Taxonomy of most important impervious surface change detection techniques

Table 1-1

Hybrid techniques

Categories	Change detection approach	Change detection task	Number of input ISF	Final result	Reference
1. Hybrid technique	Visual interpretation and image subtraction	Monitoring spatio-temporal of impervious surface	Two images	Urban change maps at two dates	Yang et al.(2003),Yang and Liu(2005),Nowak and Greenfield(2012), Wilson and Brown(2015)
	Rule based technique along with Pixel by pixel comparison	Urban change detection	Two images	Change matrices; Urban change maps at two dates	Alberti et al.(2004), Alberti et al.(2007)
	Change Vector Analysis(CVA) and Post mapping analysis	Updating impervious surface map	Two images	A single updated map	Xian and Homer(2010)
	Geographic Information System	Spatiotemporal	Three images	A single map	Ma et al. (2014)

Table 1-2

Time Series

Categories	Change detection approach	Change detection task	Number of input ISF	Final result	Reference
2.Time Series	Multi-date classification based on the temporal rule	Leveraging the temporal information from the 34 year Landsat	More than two images	A change difference map	Powell et al.(2008)
	write memory function (RGB-impervious surface)	Urban change detection; reducing amount of data	Three images for per process	A single change map at three dates	Shahtahmassebi et al.(2012)
	Image comparison	Detecting exurban and quantifying change;produce a time series of consistent impervious surface maps; summarizing information	More than two images	Urban change maps(more than two)	Michishita et al. (2012), Sexton et al.(2013), Suarez-Rubio et al. (2012), Gao et al. (2012)
	Per pixel level comparison	Modeling urban growth	More than two images	Urban change maps; Simulation of urban growth	Jantz et al. (2003), Xian and Cran(2005), Shao and Liu(2014), Sunde et al.(2014)

Table 1-3

Modeling

Categories	Change detection approach	Change detection task	Number of input ISF	Final result	Reference
3. Modeling	Conjunction of VIS model with Fuzzy technique	Measuring neighborhood effect; Quantifying magnitude of change	Two images	Map of magnitude change at two dates	Rashed et al. (2005), Rashed(2008)
	Vegetation-Impervious Surface-Soil(VIS) model	Urban change detection; Proofing strength of VIS model	Two images	Ternary plots/urban change maps at two dates	Weng and Lu(2009), Lu et al. (2011), Phinn et al. (2002), Madhavan et al.(2001)
	Spatial variance, logistic function and classification	Characterizing morphology urban growth/urban metrics/spatial pattern of impervious surface	Two images	Urban change maps at two dates	Van de Voorde et al.(2011)

Table 1-4

Spatial Metrics

Categories	Change detection approach	Change detection task	Number of input ISF	Final result	Reference
4. Spatial Metrics	Developing metrics	Analyzing pattern of change	More than two images	Graph	Zhou et al.(2012), Kuanget al. (2013), Kuang et al.(2014), Wu and Thompson (2013), Nie et al.(2015a), Nie et al.(2015b)

Although these techniques have proven effective to some degree when applied to ISFs, several problems still exist:

(i) Most techniques are designed to visualize the expansion and re-densification of impervious surfaces (e.g. Yang et al., 2003; Yang and Liu, 2005) and quantification of such changes have not been successfully addressed. In particular, there is no standard model for quantifying impervious surface change using more than two ISF data sets, so there is a requirement to develop methods that can exploit time series images to generate a single informative and intelligent map of evolution of impervious surfaces over time (Michishita et al., 2012).

(ii) Some studies have derived thematic products (i.e. classification and urban metrics) from ISFs (e.g. Van de Voorde et al., 2011; Shahtahmassebi et al., 2012) but such products may be inappropriate because some information about the characteristics of land cover transitions could be lost in this step.

(iii) There is no systematic framework to interpret the spatio-temporal changes of impervious surfaces in conjunction of urban growth theories. Many urban growth theories have been developed using information derived from basic land cover change-detection techniques (Herold et al., 2003; Herold et al., 2005; Dietzel et al., 2005). As mentioned previously, however, these methods do not account for urban changes at the sub-pixel level, notably the process of re-densification (Yang et al., 2003). Monitoring changes in impervious surfaces can provide information on both the area and density of urban regions (Ridd, 1995), therefore explicitly linking the evolution of impervious surfaces and urban growth theories could be useful for understanding the spatio-temporal patterns of intra- and inter-urban form.

(iv) Most impervious surface change detection studies have focused primarily on the temporal dimension of ISFs. However, the spatial dynamics of the data also includes useful information that has not been fully exploited. The spatial arrangement of ISFs can provide interpretations of features with greater detail and complexity which may be treated as an additional information surface (Fan and Myint, 2014).

Therefore, the aim of this study was to explore both conceptually and with a practical example how using remote sensing of impervious surfaces in combination with a spatial and spatial statistics and urban growth theories can contribute to improving our understanding of the urbanization process.

1.1A framework for remote sensing of impervious surface growth

Cities reflect economic, environmental, technological and social processes in their dynamics, yet all are in turn profoundly driven by the evolving urban spatial structure itself (Herold et al., 2003). Research into detecting, understanding, and simulating urban growth mechanisms has a long tradition in urban planning and geography. In recent years, many frameworks based on the combination of remote sensing products and spatial metrics have been developed to quantify the spatial patterns of urban development. These frameworks, such as diffusion-coalescence (Dietzel et al., 2005), mainly measure and model transformation of non-urban lands to urban regions. However, accurate and operational quantification of urban growth still presents us with some major challenges. In general, the majority of urban growth models rely heavily on time series of thematic maps which typically consider urban areas to be homogeneous. Given the land cover heterogeneity of the urban environment this definition fails to consider important structural features particularly in urban centers. Many researchers believe that detailed spatial and contextual characterization of urban land cover has high potential to result in detailed and accurate mapping of urban

land uses and socioeconomic characteristics (Herold et al. 2005). Moreover, traditional urban growth models generally take into account urban expansion around urban regions while these frameworks may not provide information regarding physical modification in urban centers.

To minimize these problems, remote sensing of impervious surfaces was developed following the vegetation-impervious surface-soil (VIS) model proposed by Ridd (1995). According to this approach, the spatial composition of a segment of urban landscape may be classified vegetation, impervious surface and soil. This makes it possible to quantify physical transformations in urban areas. However, there are two major weaknesses in this model. Firstly, the main focus of VIS is on detecting the increasing impervious surfaces at the edge of cities while modification of these surfaces is not well addressed. Secondly, the VIS model does not provide any framework for quantifying mechanisms of impervious surface changes and their spatial distribution. To this end, we developed a hypothetical spatio-temporal model of impervious surface growth which is a function of two mechanisms, expansion and re-densification. Conversion of pervious lands to impervious surfaces around existing urban regions and in formerly open spaces within urbanized areas leads to expansion and infilling of impervious surfaces, respectively. However, re-densification is considered as the renovation or replacement of pre-existing urban infrastructure. Thus, re-densification may have two forms:

- 1) Low re-densification: where density of impervious surfaces decreases over time, for example replacing older low-rise high density urban regions with mixtures of tall buildings and green spaces;
- 2) High re-densification: where the density of impervious surface increases over time as new constructions replace remaining pervious surfaces in urban areas.

The nature and patters of expansion and re-densification are of a major concern to sustainable development. Quantification of these changes can provide insights with regard to the impacts of land use regulations, population, transportation and rapid urban development. However, few studies have investigated the expansion and re-densification of these surfaces (e.g.Rashed, 2008;Michishita et al.,2012; Saxton et al., 2013).

This paper introduces a framework for quantifying patterns of expansion and re-densification of impervious surfaces using ISFs. The suggested framework is divided into two parts: methodology and interpretation. The methodological part is based on the theoretical model for impervious surface change developed by Yang et al (2003) and the residual regression approach. Specifically, the Yang et al (2003) concept was used in the present study to build a relationship between impervious surface fractions, while regression residuals were utilized to quantify change in impervious surface fractions. With respect to the interpretation, the concept of urban growth developed by Batty and Longly (1994) and the onion model (Herold et al. 2003) were employed for analyzing impervious surface expansion. Likewise, a theoretical model for physical modification of urban areas developed by Bourne et al. (1976) was implemented to guide the interpretation of re-densification.

2. Methodology

2.1 Study area and data preparation

To demonstrate the utility proposed framework, we focused on a particular study area Kandun Town in Cixi County, Zhejiang Province, China (Fig.1). This city has witnessed rapid urbanization because it is located close to three Chinese Mega cities, namely Hangzhou, Ningbo and Shanghai. In addition, Hangzhou Bay Bridge, the longest sea bridge in China, links Kandun to Shanghai. Quantifying spatio-temporal patterns of impervious surface in Kandun Town serves as an important first step toward understanding the ecological and biological consequences of the rapidly growing city. Across the town there have been different rates and forms of urbanization that are typical of those taking place across many east coastal regions of China, therefore this is a valuable study site for the purposes of this investigation.

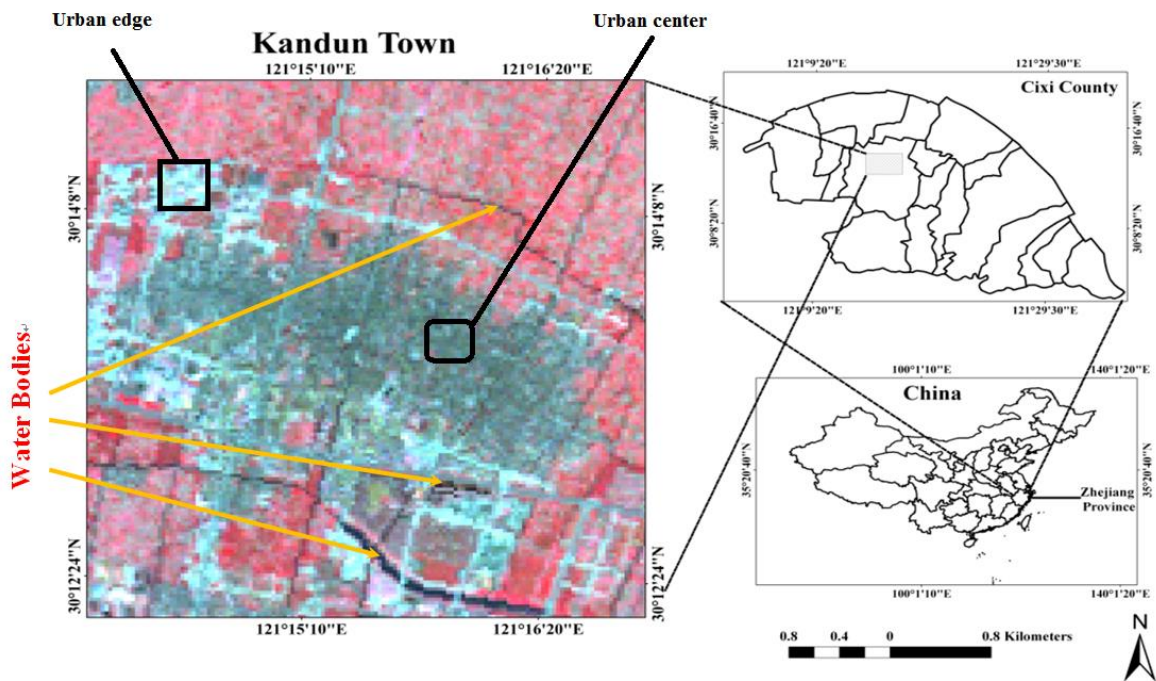


Fig.1. Study area, the satellite image is Landsat TM on 10th October 2009 in false color composite (Bands 4,3,2).

Three Landsat TM and ETM+ images (Table 2) covering the study site were acquired which had been already geometrically corrected and registered. Pre-processing of all Landsat data included clipping Kandun Town, radiometric correction, atmospheric correction and masking water bodies. The study area was clipped from the full Landsat scenes by using its administrative boundary. Then, radiometric correction was applied to those images based on published calibration coefficients and a dark-object subtraction technique was used to reduce the impact of atmospheric scattering. Water bodies (e.g. rivers and water canals) were excluded from the Landsat images to avoid confusion between these objects and impervious surfaces, by masking using an NDVI threshold.

Table 2

Summary of basic properties of the satellite imagery used.

Satellite, Sensor ¹	Date	Spatial resolution (m)	Bands used	Visibility condition
Landsat 5 TM	September 13, 1995	30	1-5,7	Clear, cloud free
Landsat 7 ETM +	November 11, 2002	30	1-5,7	Clear, cloud free
Landsat 5 TM	October 21, 2009	30	1-5,7	Clear, cloud free

¹Shahtahmassebi et al.(2014)

2.2 Data analysis strategy

The analytical approaches consisted of three parts (Fig. 2): (1) Calculating impervious surface fraction images (2), detecting changes of impervious surfaces and, (3) quantifying such changes. As the analysis combines the key components of MESMA, analysis of Regression residuals, spatial statistics (Getis_Ord) and Urban growth theories we subsequently use the abbreviation MRGU to describe this analytical framework. To provide context we compared the performance of the proposed MRGU approach with three conventional methods of change detection.

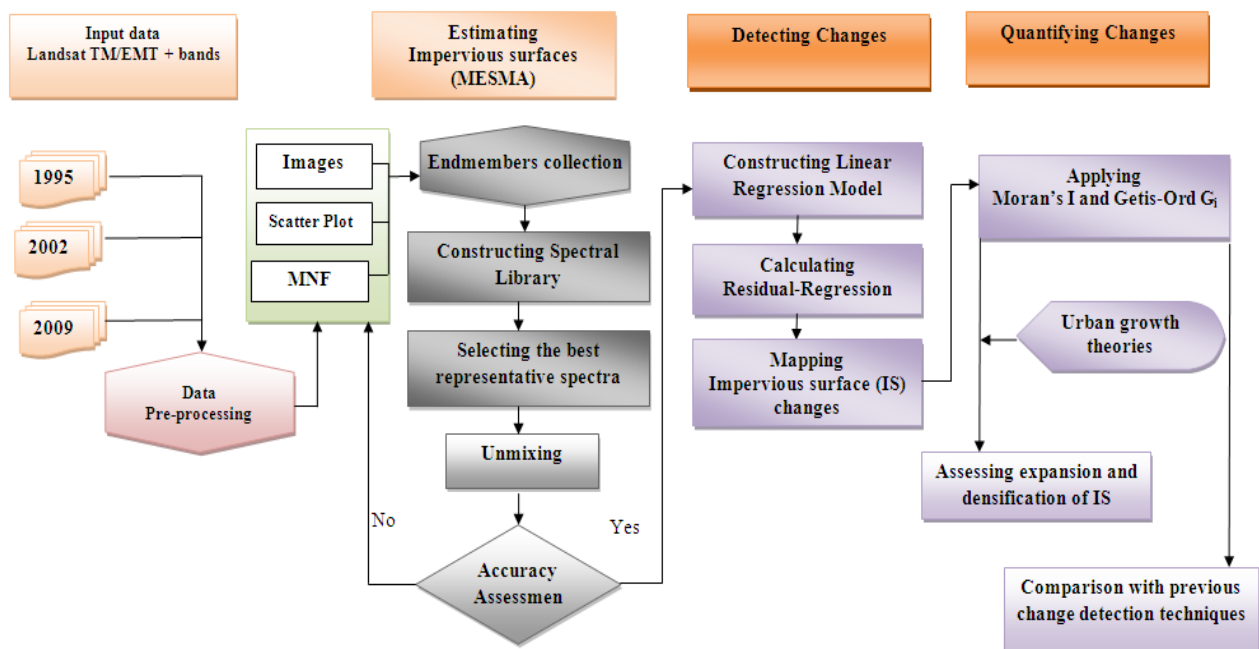


Fig.2. Diagram of the proposed workflow to characterize mechanisms of impervious surface (IS) growth from Landsat imagery (the MRGU approach)

2.3 MESMA

This technique is an extension of spectral mixture analysis (SMA) that consists of a single set of endmembers that are applied to an entire scene (Rashed et al., 2003). This model assumes a pixel's spectrum is linear combination of a finite number of spectrally distinct endmembers (Powell et al., 2007):

$$\rho'_\lambda = \sum_{i=1}^N f_i \times \rho_{\lambda i} + \varepsilon_\lambda \quad (1)$$

where ρ is the reflectance of the endmember i for a spectral band(λ), f is the fraction of the endmember, N is the number of endmembers and ε is the error term. Model fit is generally assessed using root mean squared error (RMSE), given by:

$$\text{RMSE} = \sqrt{\frac{\sum_{\lambda}^M (\varepsilon_{\lambda})^2}{M}} \quad (2)$$

where M is the number of spectral bands in an optical image. However, SMA may fail when analyzing urban regions due to the diversity of urban materials and the variety of components within the field of view(Rashed, 2008). By contrast, the MESMA algorithm allows the number of endmembers to vary for each pixel in an image. Thus it is more suitable when dealing with the mixed pixel problem in urban regions (Powell et al., 2007). This technique has been evaluated in a number of urban studies and has yielded promising results (Rashed et al., 2003; Rashed, 2008;Michishita et al., 2012). The software for MESMA (a plug-in software under ITT ENVI) is freely available via the VIPER TOOL website (Roberts, 2007). The MESMA approach was conducted based on the guidelines from previous studies (Rashed, 2008;Michishita et al., 2012;Shahtahmassebi et al., 2014) and consisted of the following steps: (1) Endmember selection; (2) Developing a spectral library; and (3)Un-mixing. These are each detailed in turn.

2.3.1 Collecting endmembers

A common approach for collecting image endmembers is selecting representative homogeneous pixels from satellite images through visualizing spectral scatter plots of image band combinations and spectral plots (Wu and Murray, 2003). In this study image endmembers were collected by using a combination of maximum noise fraction (MNF) and endmember collection spectra. MNF analysis contains two steps: (1) de-correlation and rescaling of noise in the data based on an estimated noise covariance matrix, resulting in transformed data in which the noise has unit variance and no band-to-band correlations; (2) using a principal component analysis of the noise-whitened data(Lu and Weng, 2006). In the MNF, noise is removed from the original data by using only the coherent portions, in order to enhance processing results.

The MNF procedure was applied to transform the TM 1995, ETM + 2002 and TM 2009 reflective bands into a new coordinate set. The scatter plots between MNF components 1, 2 and 3 are illustrated in Fig.3 for TM 2009 as an example, showing the potential homogeneous endmembers. We caution that the shape of MNF graph is specific to Kandun Town; indeed, different cities might generate different shape in MNF graph due to the complexity of the urban landscape.

Four endmembers were identified according to the feature spaces and their corresponding interpretations obtained from the endmember collection spectra graph based on the original reflectance data. These endmembers were (1)

vegetation cover, which represented pasture, grass and farmland, (2) soil, which highlighted soil information in agricultural lands, (3) impervious surface within the urban center, and (4) impervious surface at the urban periphery(Figure 1). The total collected endmembers are presented in Table 3. Soil and vegetation endmembers were used only in MESMA steps to accurately estimate ISF; in the remainder of the study these endmembers and corresponding fractions were excluded from the change detection investigation, as we concentrated subsequently on changes of impervious surface cover

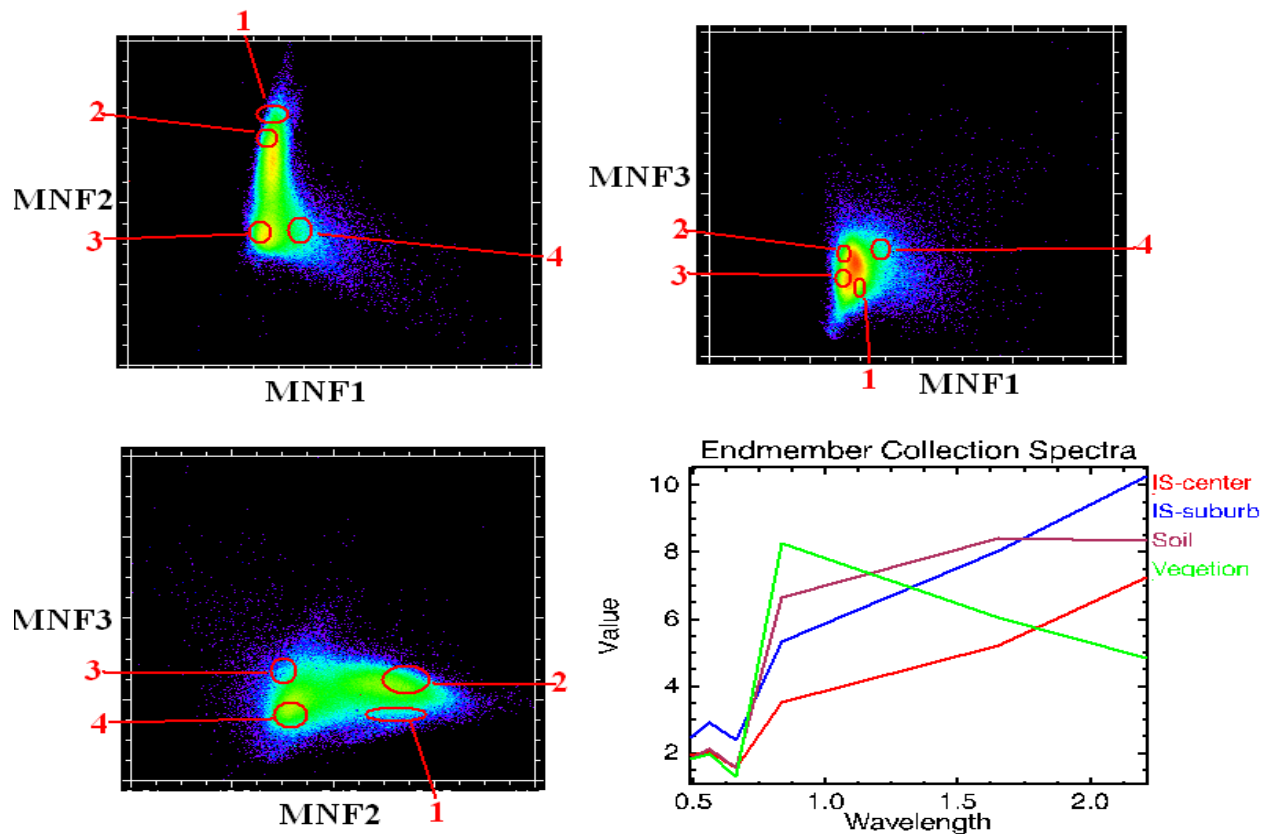


Fig.3.An example of feature space representation of the first three MNF components of the Landsat TM image from 2009. The four potential endmembers are: 1: vegetation, 2:soil, 3: impervious surface (IS) within the urban center and 4: impervious surface (IS) at the urban periphery. The bottom-right plot shows Endmember Collection Spectra of original reflectance data. For brevity, sub-classes of soil and vegetation endmembers are not shown in this figure but were analysed.

2.3.2 Selecting endmembers and developing a spectral library

The collected endmembers were imported into VIPER Tools in order to create a spectral library. To select which signatures in this spectral library were most representative of the endmembers, three optimization indices were calculated: Count Based selection (CoB), Endmember Average Root Mean Square Error(EAR) and Minimum Average Spectral Angle(MASA). The optimum spectrum has the highest CoB, lowest EAR and lowest MASA (Roberts et al., 2007). The following modeling conditions were applied to the calculation of these indices: maximum

RMSE (0.025), maximum fraction (1.05) and minimum fraction (-0.05). Finally, a new spectral library was constructed based on the pure spectra and presented in Table 3 in selected EM row.

Table 3

Number of endmembers for each category by year; Total endmembers (EM) collected in Step 1 while Selected EM were chosen following the optimization process outlined in Step 2. Classes include Impervious surface 1 (IS1), Impervious surface 2 (IS2), Soil and Vegetation cover.

Class:	Impervious surface		Soil	Vegetation Cover
Subclass:	IS 1	IS2		
1995				
Total EM	18	33	24	27
Selected EM	2	8	4	5
2002				
Total	24	37	92	28
Selected EM	3	7	6	2
2009				
Total	44	28	49	36
Selected EM	13	4	6	3

2.3.3 Un-mixing by MESMA

From the final spectral library, a subset of three spectra was chosen for the un-mixing procedure: (1) impervious surface within and around the city, (2) vegetation cover and (3) soil. In addition, parametric shade was included in this procedure. Then minimum and maximum endmember fractions were set to values of -0.1 and 1.05, respectively (Powell et al., 2007, Thorp et al., 2013) and the shade fraction was set to 0.8 according to the VIPER Tool user guide. In the last step, a range of SMA models (multi SMA models) were applied by using above spectral library. The combination of total and selected endmembers employed in the MESMA modeling is shown in Tables 4 and 5. It should be noted that four endmember models were selected over other models for the 2009 image as this improved the Root Mean Square Error (RMSE). In general, simple models such as those based on two endmembers are preferred over more complex four endmember models, except in cases where adding an endmember significantly improves RMSE (Dennison and Robert, 2003).

These models mapped each pixel in the images in terms of fractional abundance of land cover components at given point in time (Rashed, 2008). The performance of each model was evaluated using RMSE, such that if the model did not meet the threshold RMSE of less than 0.025 (Powell et al., 2007), MESMA steps should be repeated again. In this regard, the resulting mean RMSE of fraction images was 0.004, 0.007 and 0.004 in 1995, 2002 and

2009, respectively. The final products of MESMA were three fraction images for each year: Impervious surface, Vegetation and Soil.

Table 4

Detail of MESMA model parameterization for each year in Kandun town.

Year	Total EM ^a	Number of selected EM ^b	Type of combination ^c	Number of models ^d
1995	102	19	2-Endmembers	72
2002	181	18	2-Endmembers	80
2009	157	26	4-Endmembers	306

^aEM:Endmembers

^b Selected EM using techniques in step 2.

^c Number of spectral libraries added to the model.

^d The number of models was calculated as the number of impervious surface spectra \times the number of vegetation spectra \times the number of soil spectra

Table 5

Major combinations of endmember models by land cover classes with respect to year for Kandun Town.

2-endmember(1995)	2-endmember(2002)	4-endmember(2009)
IS _c +V+SHD	IS _c +V+SHD	IS _c +V+S+SHD
IS _c +S+SHD	IS _c +S+SHD	IS _{su} +V+S+SHD
IS _{ed} +V+SHD	IS _{su} +V+SHD	
IS _{ed} +S+SHD	IS _{su} +S+SHD	

IS_c refers to impervious surface in urban center, IS_{su} to impervious surface in urban edge, S to soil and V to vegetation cover and SHD to shade.

2.4 Accuracy assessment

Accuracy assessment is an important step to ensure the quality of the ISF images (Lu and Weng, 2006). Ideally, this procedure should be done by using high spatial resolution imagery which allows one to delineate borders of impervious surfaces in a way that is sufficiently precise for validating sub-pixel impervious surface extracted from medium or coarse spatial resolution imagery. However, high spatial resolution imagery may be costly and difficult to obtain for an entire study region and for each occasion in an ISF image time series, particularly for early dates (Michishita et al., 2012; Kuang et al., 2014). Due to these limitations, this study utilized a color composite aerial photograph with spatial resolution of 1 m acquired in 2009 as ground reference to assess accuracy of impervious surface fraction in 2009. The geographic extent of the 2009 aerial image covers Kandun Town with a range of land cover types, including farm land, urban vegetation, rural residential, urban residential, industrial, and farm land.

The Segment Only Feature Extraction (SOFE) of ENVI RSI 5.1 was implemented to classify reference imagery into two classes: non-impervious surface and impervious surface. The technical setting parameters of this method were: Intensity algorithm for segmentation (Scale level = 10), Full Lambda schedule algorithm for merging (Scale

level= predefined (0)) and Texture Kernel size was 3. The overall accuracy of that classification was found to be 95% based on a cross-comparison with visual assessment of samples, and this indicated that this high resolution binary image was a suitable reference for evaluating the Landsat-derived ISF images.

A 3×3 pixel (90m×90m)sampling plot was selected to reduce the impacts of geometric errors associated the both the TM image and the aerial photograph(Wu, 2004). Then six hundred twelve randomly located plots from the binary reference image were extracted with the Grid tool in ERDAS imagine 2011. Two types of error metrics, root mean square error (RMSE) and systematic error (SE), were adopted in this study to assess the accuracy of the ISF images(Wu, 2004):

$$RMSE = \sqrt{\frac{\sum_{i=1}^N (\hat{V}_i - V_i)^2}{N}} \quad (3)$$

$$SE = \frac{\sum_{i=1}^N (\hat{V}_i - V_i)}{N} \quad (4)$$

where \hat{V}_i is the impervious surface fraction modeled by MESMA for sample i ; V_i is the reference impervious surface fraction derived from the aerial photograph for sample i ; and N is the total number of samples. RMSE measures the overall estimation accuracy for all samples while SE evaluates the effects of systematic errors (e.g. over-estimation and under-estimation). The RMSE and SE were calculated for the all sample plots and for the separate urban and suburban subdivisions. Additionally, slope, intercept, coefficient of determination (R^2) of the regression relationship, and Pearson's correlation coefficient (r) were used for accuracy assessment purposes.

2.5 Quantifying change of impervious surfaces

Yang et al. (2003) were the first to suggest a theoretical framework for impervious surface change detection. The idea proposed was to correlate the impervious surface fraction in earlier time to that in the latest time. The solution that is most intuitive (most visually appealing) is attained by analyzing correlation graph. While successful for qualitative analysis, the framework may fail to generate an informative map of change in impervious surfaces. Having the basic idea of this framework, we considered that if a regression model was built among impervious surface fractions of different dates, the change in impervious surfaces could affect the performance of the regression model. Assuming the data are free of noise, these changes can be reflected in regression residuals. Consequently, the variation of regression residuals might explain growth of impervious surfaces.

The regression residuals approach quantifies the overall change in reflectance between two remotely sensed images (e.g. Landsat scenes) that may be caused by environmental factors that affect reflectance uniformly across the landscape; differences between the actual reflectance and the predicted reflectance in the successive scenes represent areas of unexpected change (Frank, 1984). Residual difference images are then created to illustrate the patterns of deviation from the regression model. In this way, the analysis of regression residuals is able to (1) apply to continuous time series imagery, (2) compress data from multiple bands into a single feature and, (3) flag abnormal changes (Chandola et al., 2009; Lein, 2012).The analysis of regression residuals has been used in several studies of land cover change in forested regions (Frank, 1984; Chandola et al., 2009; Lein, 2012).

To develop the analytical approach, we first conducted a re-examination of the analysis of regression residuals derived from a time series of ISF images and evaluated whether urban expansion and re-densification can be derived using this technique. The procedure of calculating regression residuals was as follows:

1) A linear regression model was constructed among impervious surface images:

$$\hat{Y}_{ij,is2009} = a_0 + a_1 X_{ij,is2002} + a_2 X_{ij,is1995} \quad (5)$$

Where i and j represent pixel coordinates, is stands for impervious surface fraction in different years (1995,2002,2009), and a_0 , a_1 , and a_2 are regression coefficients. X and \hat{Y} refer to the ISFs for the initial scenes and the estimated ISFs, respectively. The regression assumes that there is a linear relationship between ISFs from the third date (2009) and ISFs from the second date (2002) and the first date (1995).

2) A residual image was constructed using the difference between predicted ISF value and actual ISF value for each pixel:

$$R_{i,j,is} = Y_{ij,is2009} - \hat{Y}_{ij,is2009} \quad (6)$$

where R represents the regression residual, Y is the actual ISF.

Moreover, we assumed that between-class change could have a positive residual value because of sharp transformations of permeable lands to impervious surfaces. However, re-densification would be negative or positive due to the slight changes among impervious surface covers, restructuring built-up regions, and limitation of spatial resolution. In the results section, these assumptions are tested.

2.5.1 Spatial autocorrelation clustering (Hotspot detection)

The analysis of regression residuals is limited to the simple identification of a range of values in residual images (Frank, 1984) and it does not glean spatial information on landscape pattern. Employing measures containing spatial and textural information to the analysis of imagery can be applied as a methodology of effectively characterizing spatial patterns (e.g. Fan and Myint, 2014). To address spatial patterns in our study, two measures of spatial dependency, Global Moran's I and Local Getis_Ord (G_i) statistics were applied to the residual image.

Global Moran's I index compares the differences between neighboring pixels and the mean to provide a measure of local homogeneity (ENVI RSI 4.8). The index was computed prior to the G_i in order to obtain an appropriate lag distance for computing G_i and to minimize impacts of global spatial autocorrelation (Boots, 2002; Lanorte et al., 2013). Global Moran's I index is defined as (Moran, 1948):

$$I = \frac{\sum_i \sum_j W_{ij} (X_i - \bar{X})(X_j - \bar{X})}{(\sum_i \sum_j W_{ij}) \sum_i (X_i - \bar{X})^2} \quad (7)$$

Where N is the total number of pixels, X_i and X_j are residual ISF values for pixels i and j (with $i \neq j$), \bar{X} is the average value, and W_{ij} is an element of the weight matrix indicating the neighbor relation between i and j . Selecting the spatial neighborhood window is critical. Consequently, a queen's contiguity rule (8 surrounding pixels) was used to define the weights (Lanorte et al., 2013). The result of global Moran's I revealed that the optimum lag distance was 2 pixels in which maximized Moran's I and captures image spatial autocorrelation.

The Getis_Ord (G_i) statistic identifies hotspot regions i.e. areas where very high or very low values occur near one another (Getis and Ord, 1992). It is defined as:

$$(d) = \frac{\sum_{j=1}^n w_{ij}(d)x_j - W_i^* \bar{x}}{s[W_i^*(n - W_i^*)/n - 1]^{1/2}} \quad (8)$$

where x_j denotes the variable value of a pixel at location j , \bar{x} and s are mean and standard deviation, respectively, of all pixels in the entire image and $W_i^* = \sum_{j=1}^n w_{ij}(d)$. $\{w_{ij}(d)\}$ is a binary spatial weight matrix. A value of 1 is assigned to pixels within distance of d around the center pixel and a value of 0 is assigned to other pixels. The optimal lag distance obtained by Global Moran's I was used for computing G_i .

2.5.2 Conventional change detection techniques

The time series of three ISF images were visually interpreted. The possibilities for detecting modifications to impervious surfaces were examined together with the capability to visually interpret the processes of urban expansion and re-densification. The results of this visual interpretation are presented before those of the proposed MRGU approach, in order to provide some context.

The results of the MRGU approach were compared directly to two quantitative detection techniques. Two binary thematic maps, which included impervious and pervious surfaces classes, were generated by applying a multispectral land cover classification to the first and last Landsat images of the study site. As this process was separately performed for each year, the resultant image-to-image comparison enabled an analysis of impervious surface expansion. More information about this procedure has been provided by Yang et al.(2003). Furthermore, image differencing change detection was applied to the two ISF images from 1995 and 2009. The result was stored as a new ISF change image which had a potential range of values of -100 to 100%. Further information regarding image subtraction and other change detection methods can be found in Yang and Liu (2005).

3. Results and Discussion

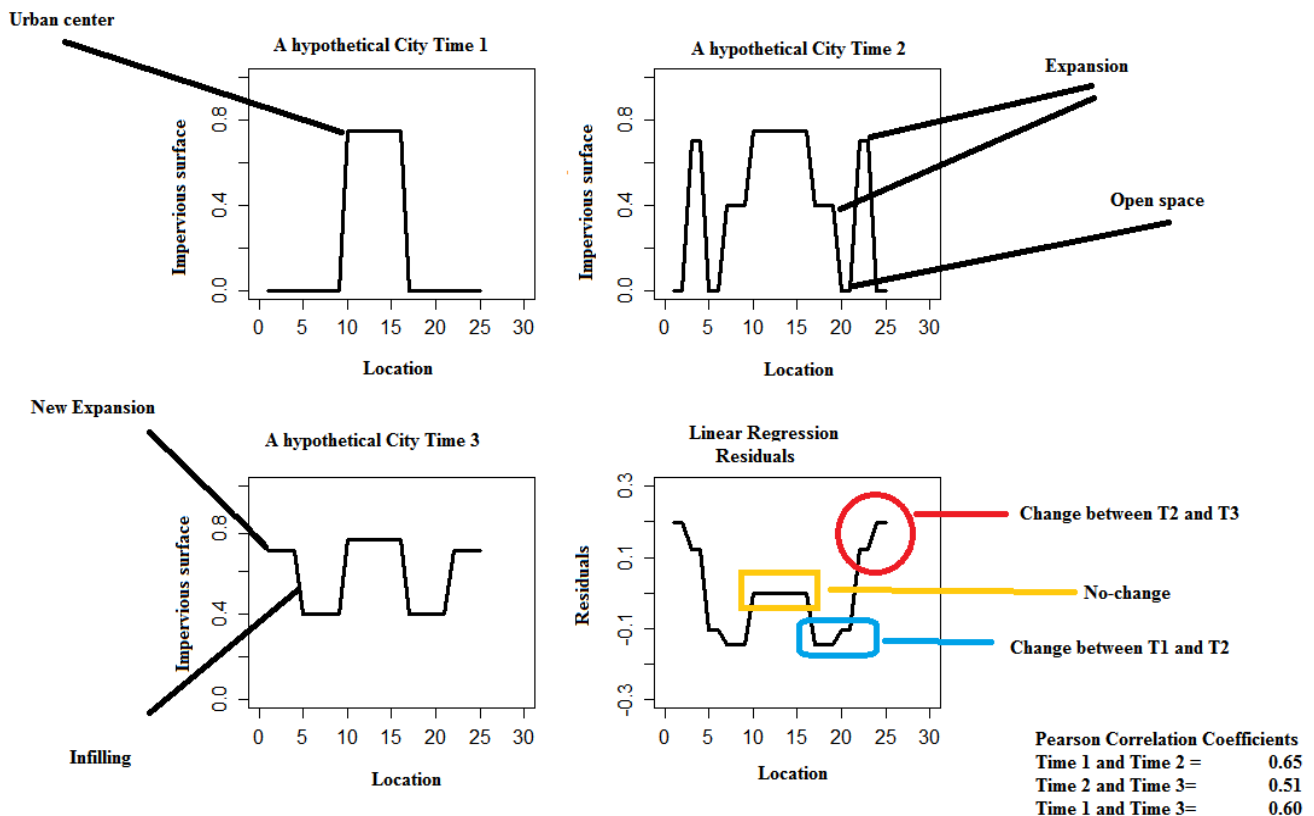
3.1 Pre-experiment

We identified two conceptual situations to examine the regression residual results.

Scenario No. 1 (Impervious surface expansion): We hypothesized an increase in the percentage of impervious surface in (infilling) and around the urban center (expansion). In this scenario, we assumed that the impervious surface of urban center had not changed over time. We also considered correlation (or linear relationship). This scenario is based on tree rings (Batty and Longly, 1994) and the onion model (Herold et al., 2003). These models hypothesize that urban growth starts with expansion around an urban seed, then new development is allocated around the existing urban center.

The results indicated moderate correlation among impervious surface fractions. Moreover, our finding showed that residual values increase and decrease over time. Accordingly, expansion and filling of impervious surface in Time 3 led to the proliferation of residuals while expansion in Time 2 generated negative residuals. Residuals of the urban center were represented by very small values close to the zero because it did not change over time (Fig.4).

Fig. 4. Residual Regression – impervious surface under Scenario 1.



Scenario No. 2(Re-densification and continuing expansion): This conceptual model postulates modest change in the percentage of impervious surfaces in urban centers and an increase in percentage of these covers in the urban periphery. We also considered correlation (or linear relationship). This scenario is based on the Bourne model (Bourne, 1976), neighborhood effects (Rashed, 2008), and restructuring of towns at the county level in China (Han, 2009). Our findings based on regression residuals support these studies: impervious surfaces in already urbanized areas may decrease or increase over time due to the restructuring process (Fig.5).

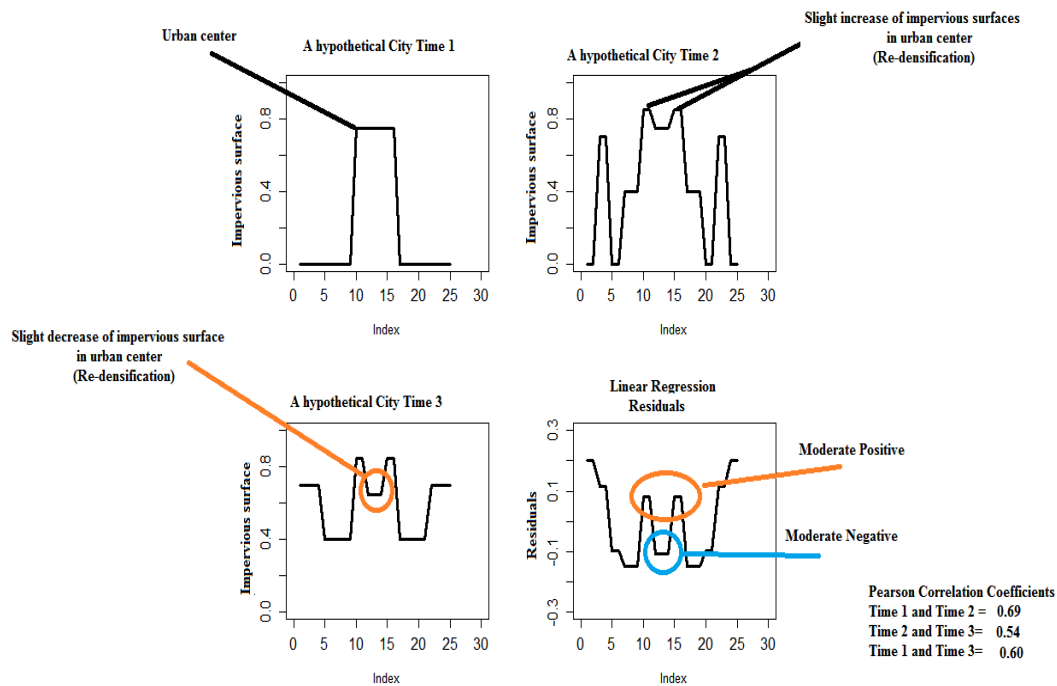


Fig. 5. Residual Regression – impervious surface under Scenario 2.

The different residual signatures for these different scenarios can enable us to identify and perhaps explain the mechanism of impervious surface changes. However, the performance of this approach depends on the structure of urban regions in the study areas and our ability to accurately capture impervious surface fraction at appropriate spatial scales (Rashed, 2008).

3.2 Accuracy Assessment

The accuracy of modeled fractions was assessed by the slope, intercept, and R^2 values associated with relationship. In an ideal case, when the modeled data perfectly agrees with the reference data, the slope of the relationship would equal one, the intercept zero, and the R^2 value would approach one (Powell and Roberts, 2010). Correlation between reference and modeled fractions was high for impervious surface fraction, with a slope of 0.99, Pearson's correlation coefficient (r) of 0.84 and R^2 equal to 0.7. Descriptive statistics of the reference and modeled fractions are presented in Table 6 and Table 7, respectively. Accordingly, strong correlation can be observed between reference ISF and modeled ISF.

Results indicate that the MESMA model has a promising accuracy in estimating ISF, with an overall RMSE of 14.17 for all sample areas (Table 7). Further, the analysis of systematic error indicates that no significant estimation bias exists for all sample areas ($SE=-3.1\%$). Residual analysis also indicated this model seems to both over-estimate and under-estimate slightly impervious surface fraction in medium developed areas (60-80%) (Figure 7-b). Also, the standardized residual showed that about 95% of data fall between -2 and +2 (Fig. 6c). It also confirmed that the possible outliers are located in the medium developed areas (60-80%).

Table 6. Summary measures for reference and modeled fractions

	Reference fraction	Modeled fraction
Minimum	0	0
Maximum	0.99	0.96
Mean	0.48	0.45
Standard Deviation	0.21	0.25

Table 7. Accuracy assessment

Metrics	
Slope	0.99
Intercept	-0.02
R ²	0.70
Pearson's r	0.84
RMSE	14.17
Bias(SE)	-3.1%

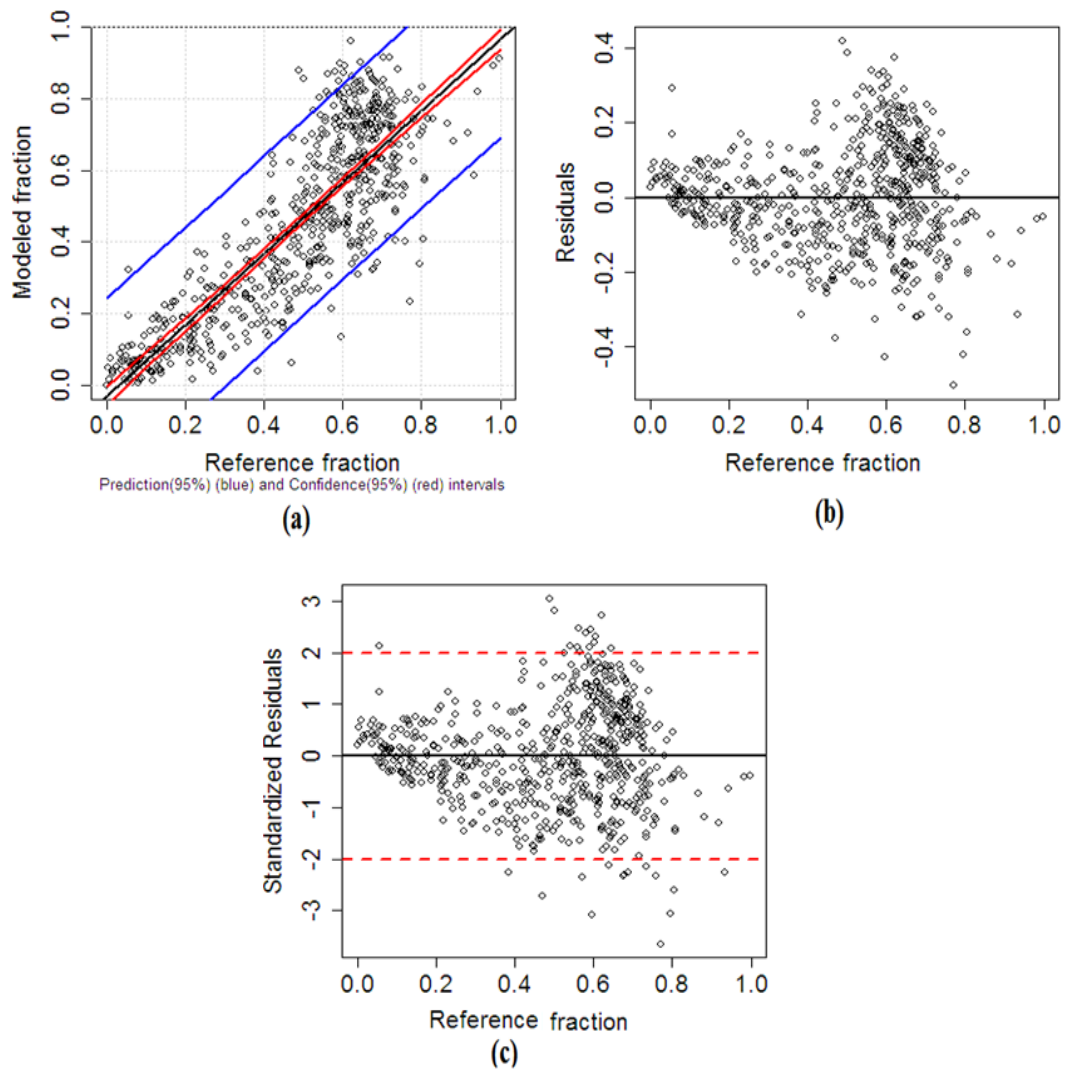


Fig. 6. Comparisons between reference and modeled fractions: (a) correlation plot, (b) regression residuals, and (c) Standardized residuals.

3.3 Visual interpretation of ISF images

The ISF images for 1995, 2002 and 2009 are illustrated in Fig.6, where impervious surface cover is represented continuously with a sequential color scheme. There was a strong correlation among these images (Table 8) which could confirm the hypothesis of Yang et al. (2003) .

By comparing across the maps, the spatial distribution of impervious surface growth between 1995-2002 and 2002-2009 can be well perceived. It is clear that the considerable increase of impervious surfaces is found around the edges of the urban center and along the developing road network, representing urban expansion. There is also a substantial increase of the percentage of impervious surface cover within the urban areas, representing densification or re-densification. In addition, the frequency histogram confirms growth of impervious surface pixels frequency, especially in high fraction of IS (>0.5) in 2009 while this year witnessed considerable decrease of low- impervious

surface pixels (>0.4)(Fig.8). Thus this visual interpretation of the ISF images provides some indication of the spatial extent and magnitude of changes in impervious surface cover, but this approach fails to adequately quantify and map the expansion and re-densification processes that have taken place.

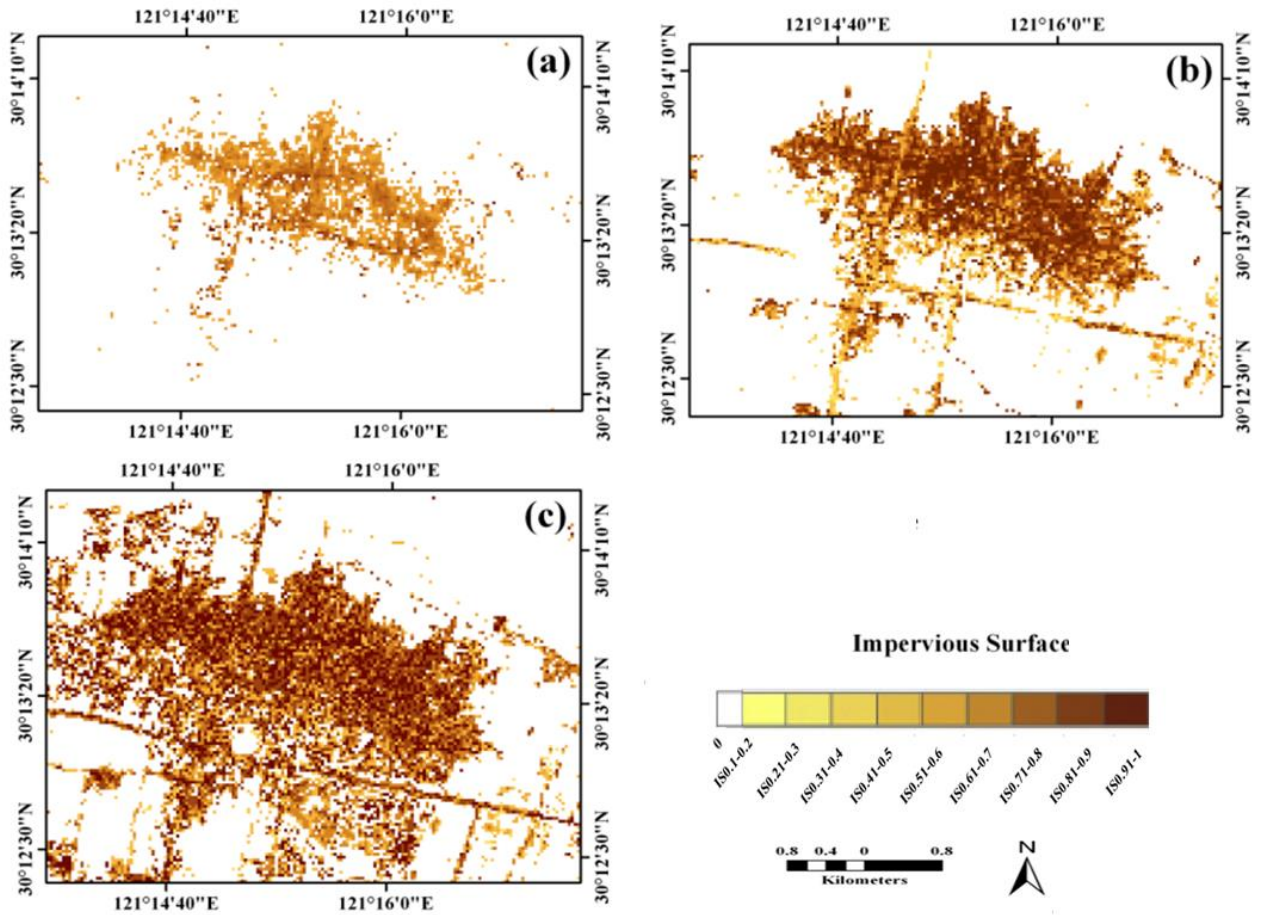


Fig.7.ISFs of Kandun Town in (a)1995, (b)2002 and (c) 2009.

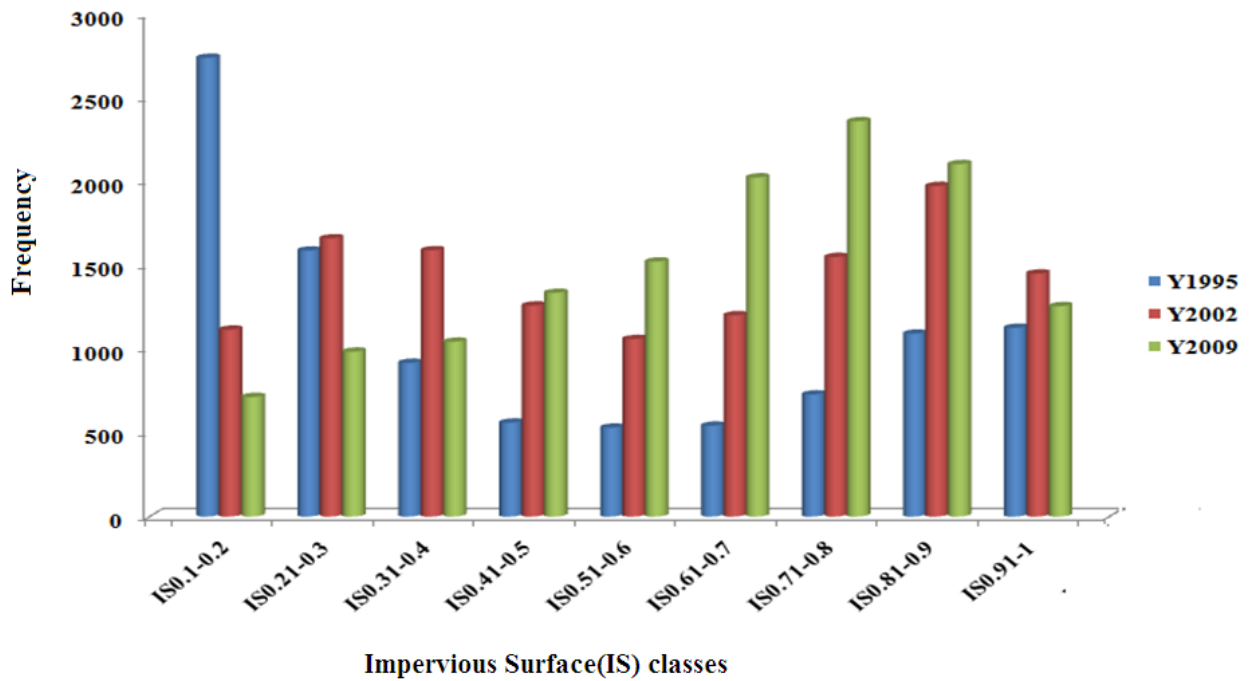


Fig.8. ISFs of Kandun town in (a)1995, (b)2002 and (c) 2009. The histogram was calculated based on the original range of impervious surfaces.

Table 8 Correlation among impervious surfaces

Correlation	IS1995	IS2002	IS2009
IS1995	1		
IS2002	0.80	1	
IS2009	0.65	0.77	1

3.4 Change detection with the MRGU approach

3.4.1 Analysis of regression residuals

When the ISF 2009 image was regressed against the ISF 2002 and 1995 images the linear least-square model generated was:

$$\text{ISF}_{2009} = 0.09 + 0.71 \times \text{ISF}_{2002} + 0.11 \times \text{ISF}_{1995} \quad (9)$$

Table 9 Regression information

Coefficients		Standard Error	t value	Pr(> t)	
Intercept	0.09	0.0018	51	<2e-16	***
ISF2002	0.71	0.0067	106.5	<2e-16	***
ISF1995	0.11	0.0076	14.6	<2e-16	***
		R-square	60%		

Significant codes: 0 '***' 0.001 '**' 0.01 '*'

The residual image of this regression is illustrated in Fig.9 (a) . A time series of Landsat false-color composite images are provided for some sample areas, to demonstrate how the residual image has responded to different forms of surface change. The residual image can also be compared with the time series of ISF images (Fig. 8), to aid interpretation. Such comparisons confirm that the expansion of impervious surfaces is highlighted by high positive values in the residual image, while the re-densification of urban areas has generated negative or moderate positive residual values. For example, in Fig.9 (a) the vertical set of Landsat images shows an area of expansion towards the edge of the town dominated by the conversion of pervious to impervious surfaces. This is where former agricultural and has been used for urban development, which generates predominantly large positive values in the residual image. The horizontal set of images covering part of the urban center illustrates an area that has experienced re-densification, where a continual cover of buildings and roads has been replaced by high rise constructions interspersed with some green spaces, generating largely negative values in the residual image.

It could be anticipated that both changes expansion and re-densification could generate positive values in the residual image because both processes can lead to an increase in the area and density of impervious surfaces. However, the behavior of the regression residuals observed in this study (Fig.9a) may be attributed to the mechanism of change (sharp and slight) in impervious surfaces and its corresponding location. In order to verify this, a profile of ISF values of across Kandun Town was extracted from the 1995, 2002, and 2009 ISF images and then superimposed (Fig.9b). The results confirmed that the urban core witnessed a slight overall increase of impervious surfaces during the whole period, which is particularly evidence in the area covered by the red arrow in Fig.9b. However, a sharp increase in ISF occurred in the urban periphery during short period, for example between 2002 and 2009 as highlighted by the black arrows in Fig.9b. These results were consistent with the findings of Ridd (1995) and

Michishita et al. (2012), who demonstrated that impervious surfaces increase sharply in the edge of developing cities in contrast to the central parts.

However, care must be exercised about observations of a decrease of impervious surfaces over time in the urban center, thereby generating negative values in the residual image. This may be an artefact of the limited spatial resolution of Landsat data and the challenges of measuring impervious surfaces in urban centers using Landsat have been recognised (Rashed, 2008; Shahtahmassebi et al., 2014). In addition, spectral resolution can affect the performance of endmember-based techniques (such as MESMA) (Weng, 2012). Therefore, given the heterogeneity and complexity of urban impervious surface materials, the spectral resolution of Landsat sensors may limit the ability to capture subtle changes in such regions. Nevertheless, the analysis of regression residuals as demonstrated in this paper does provide an ability to summarise and quantify the distribution and magnitude of impervious surface changes that have occurred through a time series of ISF images.

Finally, Kandun Town was selected to test the statistical model. This means all the estimated model coefficients are specific to this town. Thus, the model coefficients would not be directly transferrable to other places. However, the procedures undertaken and the general relationships observed in this research should be transferable.

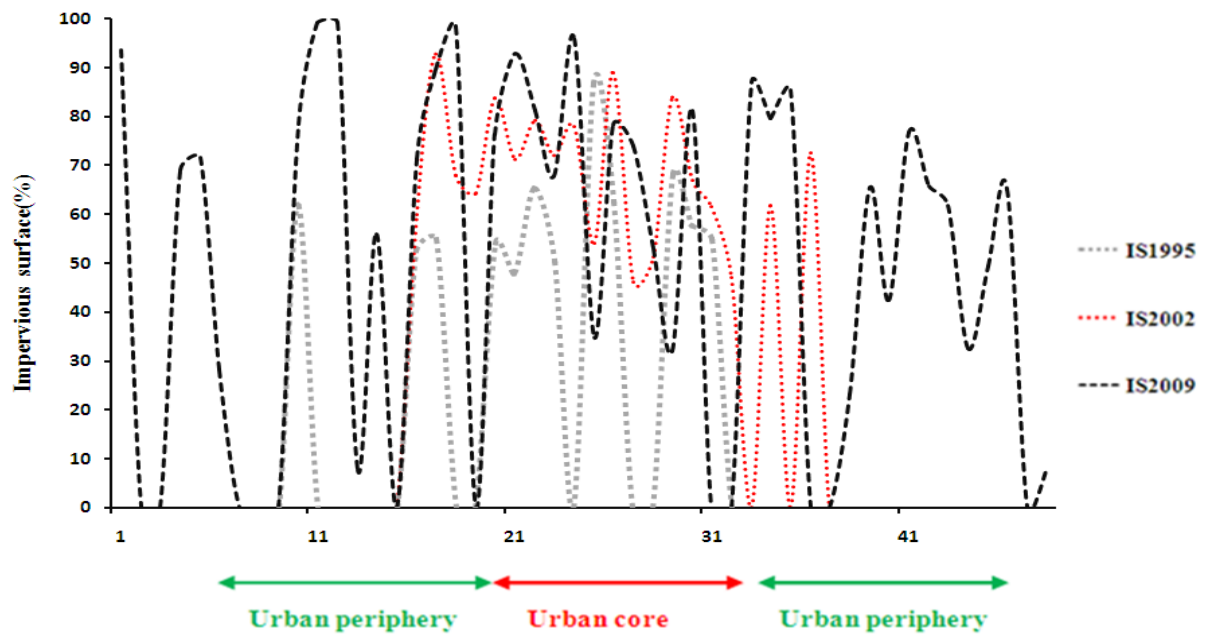
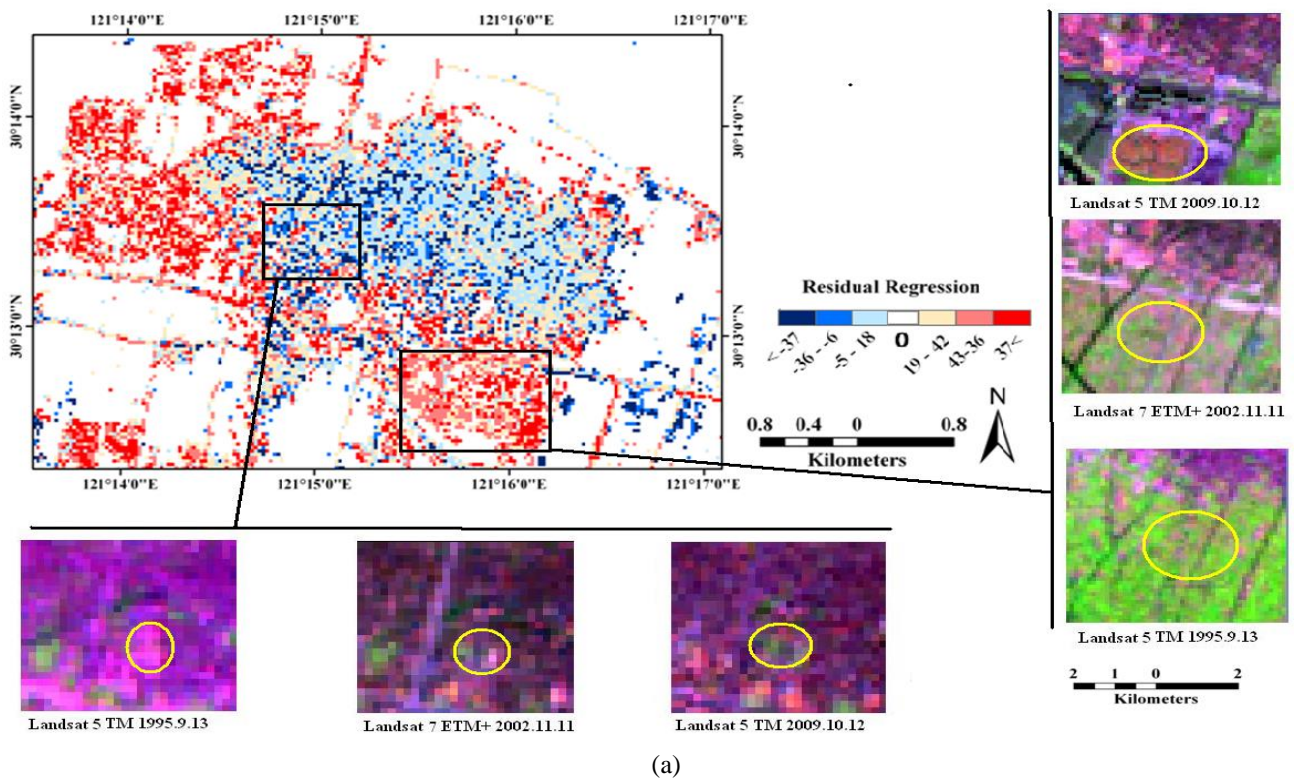


Fig.9.a)Residual image based on the ISF 1995,2002 and 2009. Zero(0) is background(non-impervious surface) in this figure. Also scale 18 is positive. Residual image were compared with color composite(Bands 7,4,3) of Landsat images in different years. **b)**Vertical profiles of impervious surface changes

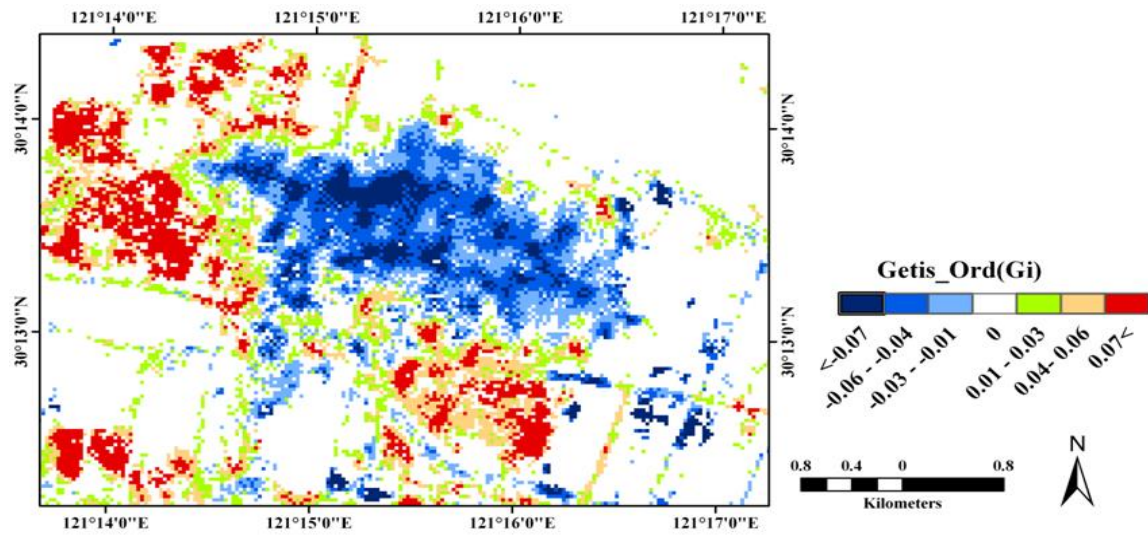
3.4.2 Spatial statistical analysis







Spatio-temporal variations of impervious surface growth are illustrated in the outputs of the Getis_Ord (G_i) analysis of the residual image in Fig.10. In order to interpret this output a profile of G_i values from across Kandun Town was superimposed upon profiles of ISF values from 1995, 2002 and 2009 (Fig. 12). This information was used to determine appropriate thresholds for differentiating and mapping re-densification and expansion processes based on G_i value (Fig.10-legend). The results suggest that G_i behaved in concert with impervious surface changes over whole period. In this regard, a dramatic increase of impervious surface generated high positive G_i values and this was generated particularly by the transition to the 2009 ISF image. Hence, expansion could be defined as those regions that had G_i values greater than 0.05 and these were predominantly located in the suburban regions. Where ISF values changed slightly over the whole period (1995 through 2002 to 2009) this produced negative G_i values which were mainly in the urban center. Therefore, re-densification could be characterized by G_i values less than 0 which were mainly located within existing urban regions. Re-densification could also be divided into two subclasses depending upon the direction of transitions in ISF values:

1) Low re-densification: where the amount of impervious surface decreased over the period of study. This subclass had G_i value between -0.03 and -0.05(e.g. Fig. 11 datapoint No.26).

2) High re-densification: where the amount of impervious surface increased over the whole period (i.e. 1995-2002-2009). This change had G_i values of less than -0.07(e.g. Fig. 11 data point No.21).

The change map generated by the MRGU approach provides useful information with which to infer the mechanisms of impervious surface change that have taken place over the time series of Landsat images. For instance, Fig.11 clearly shows areas that have witnessed rapid development over time with the significant changes from pervious lands to impervious surfaces being indicative of expansion processes. This is in contrast to other areas with much lower amounts of change experiencing re-densification due to the urban redevelopment.



Color	Getis_Ord(Gi)	Type of change	Year-IS (%)	Year-IS (%)	Year-IS (%)	Location	Function
	0.07<	BCL	1995-0	2002-0	2009-Increased	Around-existing urban regions	Expansion
	0.04-0.06	BCL	1995-0	2002-0	2009-Increased	Around-existing urban regions	Expansion
	0.01-0.03	BCL	1995-0	2002-0	2009-Increased	Around-existing urban regions	Expansion
0		BK(non-impervious surface)					
	-0.02- -0.04	WCL	1995-0	2002-Increased	2009-Increased	Within-existing urban regions	Re-densification
	-0.05- -0.07	WCL	1995-Increased	2002-Increased	2009-Decreased	Within-existing urban regions	Re-densification
	-0.08 >	WCL	1995-Increased	2002-Increased	2009-Increased	Within-existing urban regions	Re-densification

BCL: Between-Class change(expansion); WCL: Within-Class change(re-densification); BK: Background; IS: Impervious surface

Fig.10. Summary of modifications of impervious surfaces(over 1995,2002 and2009) using the Getis_Ord(Gi) index.

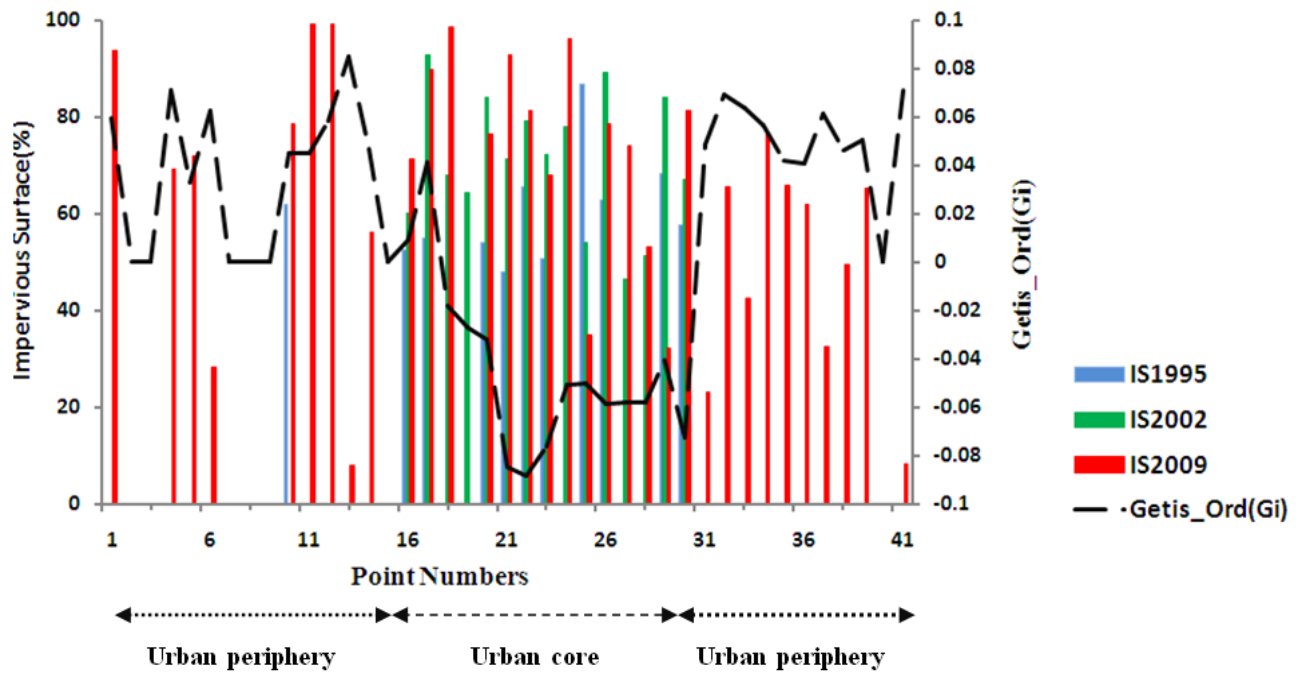


Fig.11.Profile of changes in the G_i index across the study site along with profiles of ISF values from 1995, 2002 and 2009 along the same transect.

3.5 Interpreting changes in the context of urban growth theory

In this study, using the MRGU we observed two mechanisms of impervious surface growth: expansion in peripheral areas of Kandun town and re-densification in the town center. In terms of expansion, results showed that G_i was low for the urban center that was developed before 1995 (Fig.11, dark blue). Later, the urban core was surrounded by the first ring of impervious surface growth that expanded between 1995 and 2002 (Fig.11, light blue). New urban expansion was characterized by positive G_i values which resulted from the allocation of new development around the former rings in the latest period (2002-2009) (Fig.11-a, orange color). This pattern of growth could be explained in the light of two classical urban growth models: tree rings (Batty and Longly, 1994) and the onion model (Herold et al., 2003). These models hypothesize that urban growth starts with expansion around an urban seed, then allocating new development around the existing urban center. In general this process leads to the progressive conversion of pervious land covers to impervious surfaces.

The second form of growth was re-densification in the center of Kandun Town due to the within-class change (redevelopment) of existing impervious surfaces. Low magnitude G_i values highlighted this type of modification, suggesting that impervious surfaces changed modestly or decreased in Kandun Town center during the study period. This pattern of growth could be explained by using the “thinning out” stage in the Bourne model (Bourne et al, 1976) which suggested that as part of their evolution cities undergo phase in which dense urban structures (e.g. single-family residential dwellings) are replaced by modern urban structures (hi-rise buildings). Indeed, this process corresponds with the widespread motivation of policy makers in small towns in China to promote construction of tall buildings in order to demonstrate the advanced economy in their towns (Han, 2010).

3.6 Comparative analyses with other techniques

Fig.12 shows the outputs from traditional alternatives to the proposed MRGU approach. The thematic maps (Fig 13-a) represent the urban area as a binary map of impervious and pervious surfaces. Thematic maps of impervious surfaces have been extensively used for urban growth studies (e.g. Batty and Longly, 1994;Herold et al., 2005; Dietzel et al., 2005) and do provide an overall representation of urban growth. However, despite the progress made in understanding and managing urban landscapes based such maps, there are many situations where these maps fail or are, at best, sub-optimal. In particular, the thematic maps do not accurately represent the considerable spatial heterogeneity of urban regions. When urban landscapes are represented by a discrete land cover class this may result in the loss of internal heterogeneity (Myint and Lam, 2005;Herold et al., 2005) and this may lead to a loss of information about more subtle but spatially extensive dynamics in impervious surfaces which occur particularly within urban centers.

By contrast, the change detection techniques based on the use of ISF images could mitigate this limitation. For instance, by means of visual interpretation of two ISF images (Fig.12b) or the differencing (subtraction) of ISF images (Fig.12c) the continuous scale of impervious surface variation enables us to readily observe both the expansion and re-densification of urban areas. However, in comparison to the two former methods, the outputs of the proposed MRGU approach (Fig.11) have a range of advantages. This approach produces a single change map from three impervious surface images of 1995, 2002 and 2009, thus providing an informative and appropriate representation of the evolution of impervious surfaces over time. Thus rather than providing a comparison of two image dates, this approach is able to efficiently incorporate information from a time series of images. Furthermore, the MRGU is not only able to visualize clearly the spatial distribution of urban expansion and re-densification but it also quantifies these mechanisms, as demonstrated in section 3.2.2.

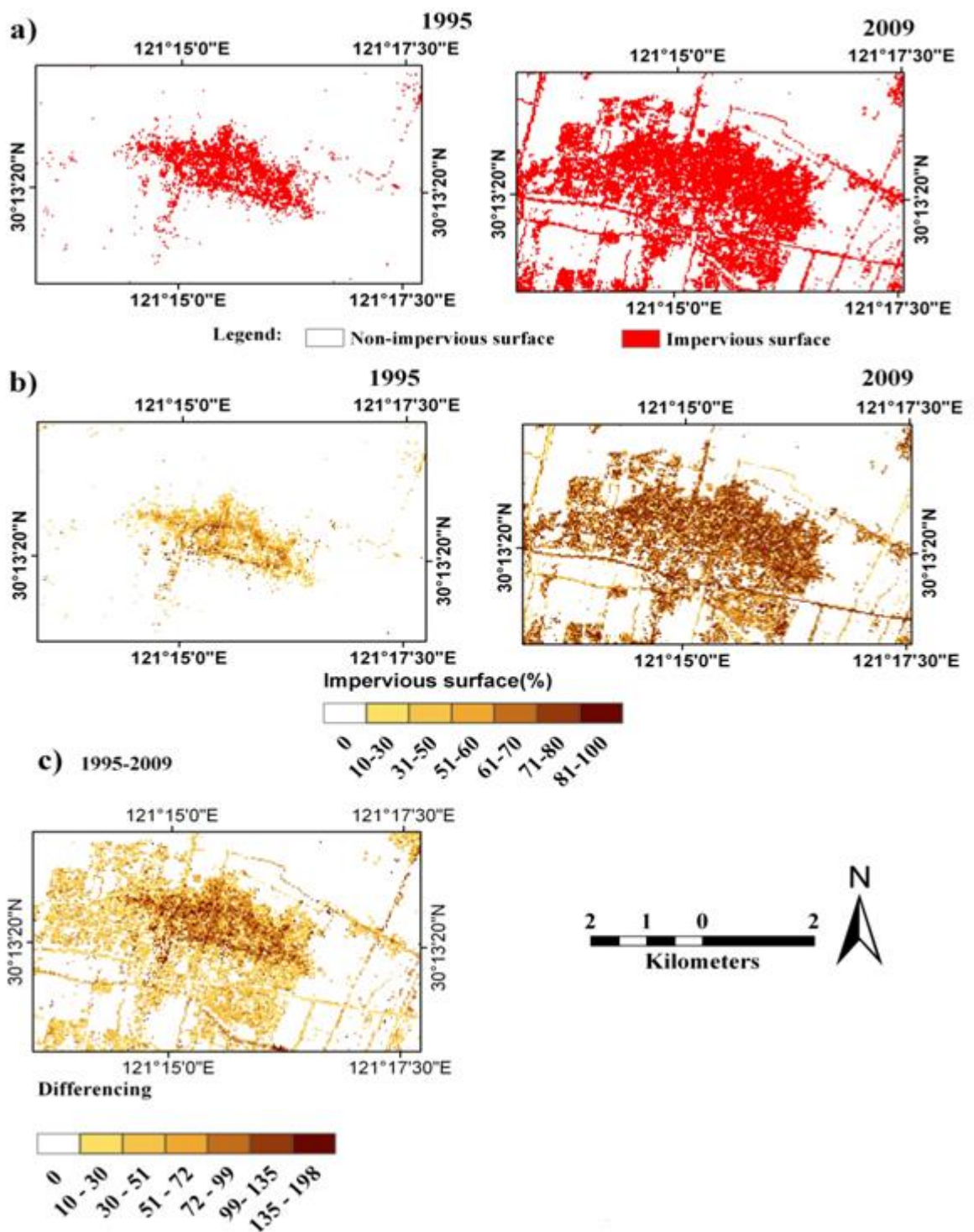


Fig.12. Evaluating the performance of traditional change detection based on (a)thematic maps; (b) visual inspection of ISF images; (c) differencing (subtraction) of ISF images.

3.7. Future of remote sensing of impervious surface growth

Effective monitoring of the evolution of impervious surfaces is an important goal for remote sensing applications in urban studies; if achieved this could contribute significantly to the field of sustainable urban planning (Weng, 2012). To this end, we have provided a summary of change detection techniques based on ISFs and developed a new technique to quantify urban expansion and re-densification. While our results were encouraging, there are several challenges which need to be addressed in future studies. Land cover compositions in urban regions are more complex with a range of different materials to those in other land covers (Powell and Roberts, 2010). Hence, this may restrict the accuracy of the ISF data derived from urban areas which, in turn might limit the effectiveness of detecting urban expansion and re-densification from satellite imagery. While many studies have provided insights into the impacts of spatial resolution and spectral resolution of satellite imagery on mapping impervious surfaces (e.g. Weng, 2012), few have concentrated explicitly on the importance of spatial and spectral resolutions in monitoring impervious surface dynamics. In particular, these characteristics could be crucial for quantifying re-densification in urban centers, a limitation that we faced in this research. The method used herein, based on Landsat data is inappropriate to generate fine resolution change maps by using ISF images. In this respect, what is required is an approach that builds upon the concept of time series super resolution mapping which has been proposed by Atkinson(2013). Nevertheless, these limitations raise three fundamental questions about monitoring change and evolution of impervious surfaces:

1- How should we assess the accuracy of time series of ISF images?

2-What are the spatial resolution requirements for measuring re-densification and expansion of impervious surfaces through time series of ISF images?

3- Which methods would be best suited for detecting fine resolution changes in ISFs over time?

Furthermore, while much research has been published on mapping impervious surfaces and detecting impervious surface changes, few studies have suggested a systematic and comprehensive framework for remote sensing of impervious surfaces growth. Based on the literature review and our findings, we propose the following framework which can be used as a guideline for measuring the growth of impervious surfaces. The framework depicted in Figure 13 shows possible steps and introduces 8 major directions which might be addressed in future research on evolution of impervious surfaces.

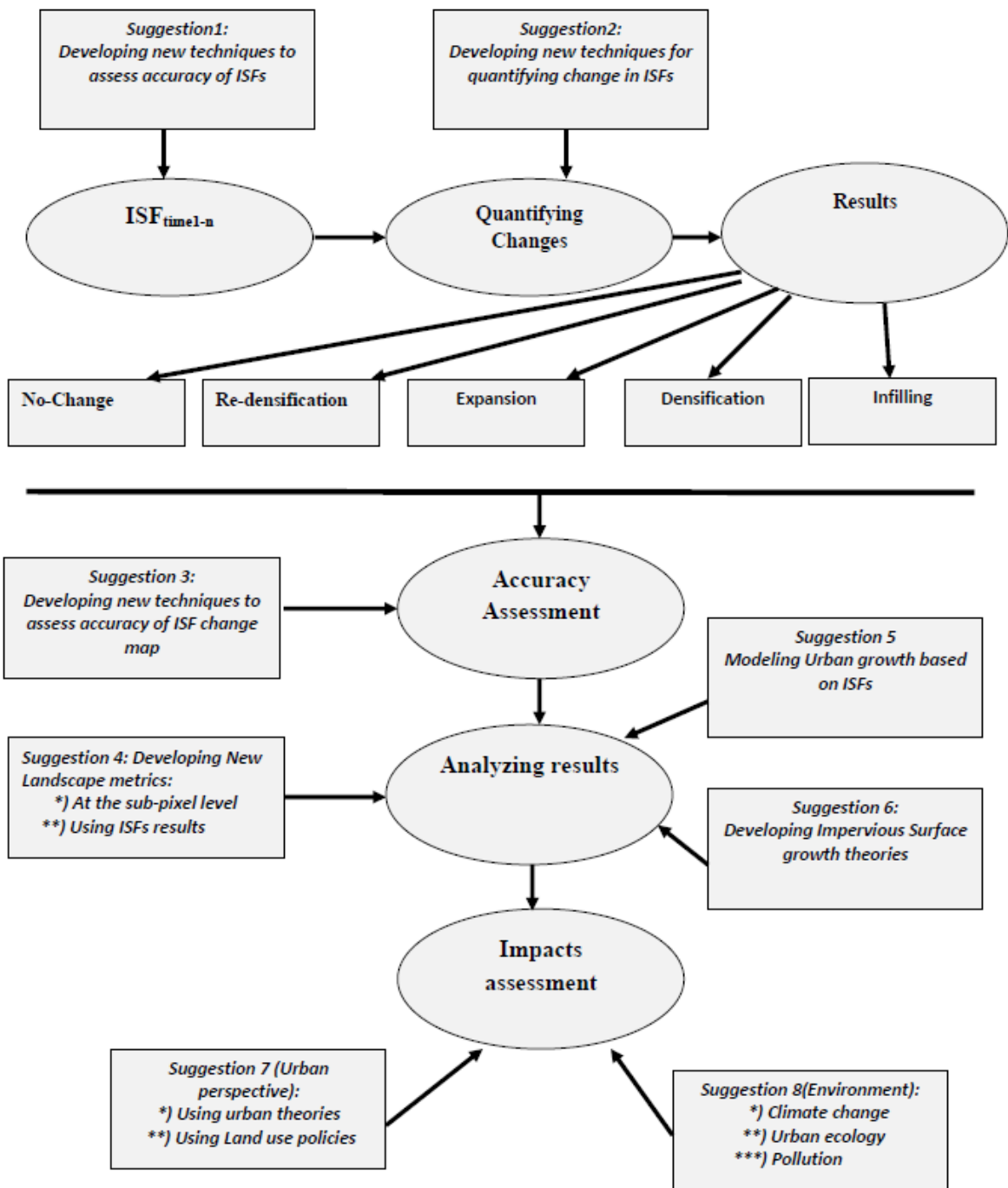


Fig.13.A possible framework for remote sensing of impervious surfaces growth and suggestions for beneficial areas of future research.

4. Conclusion

This study proposed the MRGU approach that integrates time series of ISF images, analysis of regression residuals, spatial statistics and urban growth theories to identify and understand the magnitude and spatial distribution of impervious surface changes. Our results confirmed that the G_i statistic applied to ISF regression residuals is effective for discerning change of impervious surfaces and for compressing this information into a single, statistically

effective measure which can be mapped. This approach detects two mechanisms of impervious surface growth–expansion and re-densification at the same time compared to the conventional change detection techniques which tend to focus on expansion only. This study has generated advances in the practical aspects of monitoring impervious surface growth dynamics from remote sensing and helps to establish linkages between the empirical observations, mechanisms of impervious surface change and urban growth theories. Hence, the proposed MRGU framework is significant for both remote sensing and urban sciences. This analysis indicated that quantifying change in urban centers is difficult and future research needs to focus on developing the MRGU approach by improving the accuracy of ISF retrievals using time series high resolution satellite imagery, in order to further develop capabilities in quantifying the process of urban re-densification. Further, this study offers a new conceptual strategy for remote sensing of impervious surface growth. The framework consists of change detection steps and alternative avenues on this topic.

Acknowledgements

The research was supported by the Technology Support Foundation, China (2006BAJ05A02). The authors would also like to thank anonymous reviewers for their highly constructive comments on the original manuscript.

Reference

- Alberti, M., Weeks, R., Coe, S., 2004. Urban land-cover change analysis in central Puget Sound. *PhotogrammEngRemoteSensing*.70, 1043-1052.
- Alberti, M., Booth, D., Hill, K., Coburn, B., Avolio, C., Coe S., Spirandelli, D., 2007. The impact of urban patterns on aquatic ecosystems: An empirical analysis in Puget lowland sub-basins. *Landsc.Urban Plan*.80,345-361.
- Atkinson, P.M., 2013. Downscaling in remote sensing. *Int. J. Appl. Earth Obs. Geoinf*.22,106-114.
- Batty, M., Longley, P., 1994. *Fractal Cities*. Academic Press, London, UK, pp.33.
- Boots, B., 2002. Local measures of spatial association. *Ecoscience*.9, 168-176.
- Bourne, L.S., 1976. In D.T. Herbert & R.J. Johnston (Eds.), in *Social areas in cities-V1: Spatial processes and form* New York: Wiley, pp.111-158.
- Chandola, V., Banerjee, A., Kumar, V., 2009. Anomaly Detection: A Survey. *ACM Computing Surveys*.41, 1-72.
- Demarchi, L., Cheung-W.J., Ma, J., Canters, F., 2012. Mapping impervious surfaces from superresolution enhanced CHRIS/Proba imagery using multiple endmember unmixing. *J. Photogram. Remote Sens*.72,99-112.
- Dennison, P.E., Roberts, D.A., 2003. Endmember selection for multiple endmember spectral mixture analysis using endmember average RMSE. *Remote Sens Environ*.87,123-135.
- Dietzel, C., Herold, M., Hemphil, J.J., Clarke, K.C., 2005. Spatio-temporal dynamics in California's Central Valley: Empirical links to urban theory. *Int. J. Geogr. Inf. Sci*.19,175-195.
- Elvidge, C.D., Tuttle, B.T., Sutton, P.C., Baugh, K.E., Howard, A.T., Milesi, C., Bhaduri, B.L., Nemani, R., 2007. Global Distribution and Density of Constructed Impervious Surface. *Sensor*.7,1962-1979.
- ENVI RSI 4.8 Help. ITT Industries, Inc.
- Fan, C., Myint, S., 2014. A comparison of spatial autocorrelation indices and landscape metrics in measuring urban landscape fragmentation. *Landsc. Urban Plan*, 121, 117-128.
- Frank T.D., 1984. Assessing change in the surficial character of a semiarid environment with Landsat residual images. *PhotogrammEngRemoteSensing*.50, 471-480.
- Gao, F., Colstoun, De, E.B., Ma, R., Weng, Q., Masek, J.G., Chen, J., Pan, Y., Song, C., 2012. Mapping impervious surface expansion using medium-resolution satellite image time series: a case study in the Yangtze River Delta, China. *Int. J. Remote Sens*. 33,7609-7628.
- Getis, A., Ord, J.K., 1992. The analysis of spatial association by use of distance statistics. *Geogr. Anal*. 24, 189-206.
- Han, S.S., 2010. Urban expansion in contemporary China: What can we learn from a small town? *Land Use Pol*, 27,780-787.
- Herold, M., Goldstein, N. C., Clarke, K. C., 2003. The spatiotemporal form of urban growth: measurement, analysis and modeling. *Remote Sens Environ*, 86, 286-302.
- Herold, M., Couclelis, H., Clarke, K.C., 2005. The role of spatial metrics in the analysis and modeling of urban land use change. *Comput. Environ. Urban Syst*., 2, 369-399.
- Jantz, C.A., Goetz, S.J., Shelley, M.K., 2003. Using the SLEUTH urban growth model to simulate the impacts of future policy scenario on urban land use in the Baltimore-Washington metropolitan area. *Environ. Plan. B: Plan. Des*. 30,251-271.
- Lanorte A., Danese M., Lasaponara R., Murgante, B., 2013. Multiscale mapping of burn area and severity using multisensory satellite data and spatial autocorrelation analysis. *Int. J. Appl. Earth Obs. Geoinf*, 20,42-51.
- Lein, J.K., 2012. *Environmental Sensing: Analytical Techniques for Earth Observation*. Springer, (Chapter 8, pp.193-212).
- Lu, D. Weng, Q., 2006. Use of impervious surface in urban land use classification. *Remote Sens Environ*.102, 146-160.
- Lu, D., Moran, E., Hetrik, S., 2011. Detection of impervious surface change with multitemporal Landsat images in an urban-rural frontier. *J. Photogram. Remote Sens*., 66,298-306.
- Kuang, W.H., Liu, J.Y., Zhang, Z.X., Lu, D.S., Xiang, B., 2013. Spatiotemporal dynamics of impervious surface areas across China during the early 21st century. *Chin. Sci. Bull*,58(14), 1691-1701.
- Kuang W.H., Chi, W.F., Lu, D., Dou Y.Y., 2014. A comparative analysis of megacity expansions in China and the U.S: Patterns, rates and driving forces. *Landsc.Urban Plan*.132,121-135.

- Ma, Q., He, C., Wu, J., Liu Z., Zhang, Q., Sun, Z., 2014. Quantifying spatiotemporal patterns of urban impervious surfaces in China: An improved assessment using nighttime light data. *Landsc. Urban Plan.* 130, 36-49.
- Madhavan, B.B., Kubo, S., Kurisaki, N., Sivakumar T.V.L.N., 2001. Appraising the anatomy and spatial growth of the Bangkok Metropolitan area using a vegetation-impervious-soil model through remote sensing. *Int. J. Remote Sens.* 22, 789-806.
- Michishita, R., Jiang, Z., Xu, B., 2012. Monitoring two decades of urbanization in the Poyang Lake area, China through spectral unmixing. *Remote Sens Environ.* 117, 3-18.
- Moran, P., 1948. The interpretation of statistical maps. *Journal of the Royal Statistical Society*, 10, 243-251.
- Myint, S.W., Lam, N., 2005. A study of lacunarity-based texture analysis approaches to improve urban image classification. *Comput. Environ. Urban Syst.* 29, 501-523.
- Nie Q, Xu J, Liu., 2015a. Fractal and multifractal characteristic of spatial pattern of urban impervious surfaces. *Earth Sci. Inform.* 8(2), 381-392.
- Nie Q, Xu J, Man W, Sun F, 2015b. Detrended fluctuation analysis of spatial patterns on urban impervious surface. *Environ. Earth Sci.* 74(3), 2531-2538.
- Nowak D.J, Greenfield E.J., 2012. Tree and impervious cover change in U.S. cities. *Urban For. Urban Green*, 11, 21-30.
- Parece , T.E., Campbell, J.B., 2013. Comparing Urban Impervious Surface Identification Using Landsat and High Resolution Aerial Photography. *Remote Sens.* 5, 4942-4960.
- Phinn, S., Stanford, M., Scrath, P., Murray, A.T., Shy, P.T., 2002. Monitoring the composition of urban environments based on the vegetation-impervious surface-soil (VIS) model by subpixel analysis techniques. *Int. J. Remote Sens.* 23, 4131-4153.
- Powell, R.L., Roberts, D.A., Dennison, P.E., Hess, L.L., 2007. Sub-pixel mapping of urban land cover using multiple endmember spectral mixture analysis: Manaus, Brazil. *Remote Sens Environ.* 106, 253-267.
- Powell, S. L., Cohen, W. B., Yang, Z., Pierce, J. D., Alberti, M., 2008. Quantification of impervious surface in the Snohomish Water Resources Inventory Area of Western Washington from 1972-2006. *Remote Sens Environ.* 112, 1895-1908.
- Powell, R., Roberts, D., 2010. Characterizing urban land-cover change in Brazil. *Journal of Latin American Geography.* 9, 183-211.
- Rashed, T., Weeks, J., Roberts, D.A., Rogan, J., Powell, P., 2003. Measuring the physical composition of urban morphology using multiple endmember spectral mixture models. *Photogramm. Eng. Remote Sens.* 69, 1011-1020.
- Rashed, T., Weeks, J., Stow, D., Fugate, D., 2005. Measuring Temporal Compositions of Urban Morphology through Spectral Mixture Analysis: Toward a Soft Approach to Change Analysis in Crowded Cities. *Int. J. Remote Sens.* 26, 699-718.
- Rashed, T., 2008. Remote sensing of within-class in urban neighbourhood structures. *Comput. Environ. Urban Syst.* 32, 343-354.
- Ridd, M.K., 1995. Exploring a V-I-S (Vegetation-Impervious Surface-Soil) model for urban ecosystem analysis through remote sensing: Comparative anatomy for cities. *Int. J. Remote Sens.* 16, 2165-2185.
- Roberts, D.A., Halligan, K., Dennison, P.E., 2007. VIPER Tools User Manual (Version 1.5), University of California at Santa Barbara. 91p. Available at <http://www.vipertools.org/>.
- Shao Z., Liu C., 2014. The integrated use of DMPSP-OLS Nighttime Light and MODIS Data for Monitoring Large-Scale Impervious Surface Dynamics: A case study in the Yangtze River Delta. *Remote Sens.* 6, 9359-9378.
- Suarez-Rubio, M., Lookingbill, T.R., Elmore, A.J., 2012. Exurban development derived from Landsat from 1986 to 2009 surrounding district of Columbia, USA. *Remote Sens Environ.* 124, 360-370.

- Sexton, J.O., Song, X.P., Huang, C.Q., Channan, S., Baker, M.E., Townshend, J.R., 2013. Urban growth of the Washington, D.C.-Baltimore, MD metropolitan region from 1984 to 2010 by annual Landsat-based estimates of impervious cover. *Remote Sens Environ.* 129, 42-53.
- Shahtahmassebi, A.R., Yu, Z.L., Wang, K., Xu, H.W., Deng, J.S., Li J-D., Luo, R.S., Wu, J., Moore, N., 2012. Monitoring rapid urban expansion using a multi-temporal RGB-impervious surface model. *Zhejiang Univ Sci A*. 13, 146-158.
- Shahtahmassebi, A.R., Pan, Y., Lin, L., Shortridge, A., Wang, Ke., Wu, J.X., Wu, D., Zhang, J., 2014. Implications of land use policy on impervious surface cover change in Cixi County, Zhejiang Province, China. *Cities*, 39, 21-36.
- Slonecker, E.T., Jennings, D., Garofalo, D., 2001. Remote sensing of impervious surface: A review. *Remote Sensing Reviews*, 20, 227-255.
- Sun, Z.C., Guo, H.D., Li, X.W., Lu, L.L., Du, X.P., 2011. Estimating urban impervious surfaces from Landsat-5 TM imagery using multilayer perceptron neural network and support vector machine. *J. Appl. Remote Sens.* 5, 053501.
- Sunde M.G., He H.S., Zhou, B., Hubbard J.A., Spicci, A., 2014. Imperviousness Change Analysis Tool (I-CAT) for simulating pixel-level urban growth. *Landsc. Urban Plan.* 124, 104-108.
- Thorp K.R., French A.N., Rango A., 2013. Effect of image spatial and spectral characteristics on mapping semi-arid rangeland vegetation using multiple endmember spectral mixture analysis (MESMA). *Remote Sens Environ.* 132, 120-130.
- Van de Voorde, T., Jacquet, W., Canters, F., 2011. Mapping form and function in urban areas: An approach based on urban metrics and continuous impervious surface data. *Landsc. Urban Plan.* 102, 143-155.
- Weng, Q., Lu, D., 2009. Landscape as a continuum: an examination of the urban landscape structures and dynamics of Indianapolis City, 1991-2000, by using satellite images. *Int. J. Remote Sens.* 30, 2547-2577.
- Weng, Q., 2012. Remote sensing of impervious surfaces in the urban areas: Requirements, methods, and trends. *Remote Sens Environ.* 117, 34-49.
- Wilson, C.R., Brown, D.G., 2015. Change in visible impervious surface area in southeastern Michigan before and after the "Great Recession:" spatial differentiation in remotely sensed land-cover dynamics. *Popul. Env.* 36, 331-355.
- Wu, C., Murray, A.T., 2003. Estimating impervious surface distribution by spectral mixture analysis. *Remote Sensing of Environment*, 84, 493-505.
- Wu, C., 2004. Normalize spectral mixture analysis for monitoring urban composition using ETM + imagery. *Remote Sens Environ.* 93, 480-492.
- Wu J., Thompson, J., 2013. Quantifying impervious surface changes using time series planimetric data from 1940 to 2011 in four central Iowa cities, USA. *Landsc. Urban Plan.* 120, 34-47.
- Xian, G., Crane, M., 2005. Assessments of urban growth in the Tampa Bay watershed using remote sensing data. *Remote Sens Environ.* 97, 203-215.
- Xian, G., 2007. Mapping Impervious Surfaces Using Classification and Regression Tree Algorithm in: Weng, Q. (Eds.), *In Remote Sensing of Impervious Surfaces*, CRC Press: Boca Raton, FL, USA, pp. 39-59.
- Xian, G., Homer, C., 2010. Updating the 2001 National Land Cover Database impervious surface products to 2006 using Landsat imagery change detection methods. *Remote Sens Environ.* 114, 1676-1686.
- Yang, L., Xian, G., Kalver, J.M., Deal, B., 2003. Urban Land-Cover Change Detection through Sub-Pixel Imperviousness Mapping Using Remotely Sensed Data. *Photogramm Eng Remote Sensing*. 69, 1003-1010.
- Yang, X., Liu, Z., 2005. Use of satellite-derived landscape imperviousness index to characterize urban spatial growth. *Comput. Environ. Urban Syst.* 29, 524-540.
- Zhou, B., He, S.H., Nigh, T.A., Schulz, J.H. 2012. Mapping and analyzing change of impervious surface for two decades using multi-temporal Landsat imagery in Missouri. *Int. J. Appl. Earth Obs. Geoinf.* 18, 195-206.